Technical Report
TR-16-07
December 2017

Full scale Buffer Swelling Test at dry backfill conditions in Äspö HRL

In situ test and related laboratory tests

Torbjörn Sandén
Lennart Börgesson
Ulf Nilsson
Ann Dueck

SVENSK KÄRNBRÄNSLEHANTERING AB

SWEDISH NUCLEAR FUEL
AND WASTE MANAGEMENT CO

Box 3091, SE-169 03 Solna
Phone +46 8 459 84 00
skb.se

SVENSK KÄRNBRÄNSLEHANTERING

ISSN 1404-0344
SKB TR-16-07
ID 1525657
December 2017

Full scale Buffer Swelling Test at dry backfill conditions in Äspö HRL

In situ test and related laboratory tests

Torbjörn Sandén, Lennart Börgesson, Ulf Nilsson,
Ann Dueck

Clay Technology AB

Keywords: Buffer swelling, Backfill block, Hydraulic jacks, BS test, KBP1012.

Summary

The Buffer Swelling Test (SKB project BS test) was performed in Äspö HRL as a complement to a test of backfilling a tunnel with backfill blocks. A "simulated deposition hole" with a depth of about 1.5 meter was excavated in the tunnel floor and equipped with four hydraulic jacks on the bottom of the hole, a steel plate with an outer diameter of 1.75 m resting on the jacks and a bentonite buffer block placed on the steel plate. The tunnel above the simulated deposition hole was filled with backfill blocks and pellets according to the backfill design developed within the project "KBP1003 System design of backfill" (Arvidsson et al. 2015). The buffer block was then pushed upwards by the hydraulic jacks during the test, simulating the swelling buffer from a deposition hole towards a dry backfilled tunnel. The vertical force, the displacement of the steel plate and the pressure against the rock surface were measured during the test.

The total buffer block displacement upwards was approx. 150 mm and the maximum pressure approx. 1 800 kPa was reached after 75–80 mm vertical displacement after which a residual stress of 1 200–1 400 kPa was measured.

Only two of the five sensors placed on the rock surface above the deposition hole (at different positions) registered a significant pressure increase. At the midpoint above the deposition hole, on the rock ceiling, a maximum pressure of approx. 350 kPa was registered. At the left corner, in the transition between the ceiling and the wall a pressure of approx. 300 kPa was registered.

The contact pressure between the backfill blocks was measured by special indicators (plastic films), registering the maximum pressure they have been exposed to. These indicators were placed at 41 different positions. The results from these measurements were rather inconsistent, showing a strong variation and a lack in stress reduction with distance from the floor. It is not clear whether these trends are real or a result of the method of measurement.

The backfill blocks above and around the simulated deposition hole were carefully examined during the excavation. The backfill blocks just above the deposition hole typically showed shearing at the buffer block periphery. The blocks in the three first layers above the borehole showed considerable damage, while the blocks in the next four layers had cracked in some directions. The blocks in the four uppermost layers exhibited very small damage and seemed to have been displaced rather than damaged.

The backfill block layers had a very evident "bow shape" above the deposition hole due to the larger vertical displacement in the centre than in the periphery. The outermost blocks, at the walls, seemed to have been moved somewhat outwards against the rock wall.

It seemed as if the applied load from the simulated buffer heaving had not been laterally distributed in the block stack except for in the first half of the test before maximal load was reached. Instead the backfill blocks had been sheared off at many positions. This is in agreement with the pressure film measurements but not in agreement with the low pressure measured at the roof. These observations may be a result of distinct difference in behaviour before and after block failure.

The total buffer vertical displacement, approx. 150 mm was distributed in the different parts of the backfill above the simulated deposition hole in the following way:

- The 70–90 mm thick pellet layer on the floor between the buffer block and the bottom backfill block has been compressed about 30 mm.
- The 430 mm thick pellet layer in the ceiling between the upper backfill block and the rock ceiling has been compressed about 40 mm.
- The backfill block section (compression of slots, elastic compression and movements in horizontal direction) has been compressed about 80 mm.

Laboratory measurements of the uniaxial compression strength and the tensile strength of the backfill blocks used in the field test showed that the strength was rather low compared with earlier measurements, mainly due to the low density and relatively low water content. The spreading (and

hence lower measured magnitude) of the compression stresses in the field test was also due in-part to the large granules in the bentonite. However, the average uniaxial compression strength measured in the laboratory was about 1 600 kPa, which agrees very well with the applied peak axial stress at the Buffer Swelling Test reached just before failure of many of the backfill blocks. A preliminary conclusion is that the resistance to upwards swelling can be substantially improved if the backfill blocks were made to higher density and thereby exhibit higher compression strength.

Sammanfattning

Fältförsöket “Buffer Swelling Test” (SKB projekt BS test) genomfördes på Äspö HRL som ett komplement till ett försök med återfyllning av en tunnel med återfyllningsblock. Ett simulerat deponeringshål med djupet ca 1,5 m togs upp i tunnelgolvet och utrustades med fyra hydrauliska domkrafter i hålets botten. En stålplatta med en ytterdiameter av 1,75 m med ett ovanför liggande buffertblock placerades på domkrafterna. Tunneln ovanför det simulerade deponeringshålet fylldes sedan med återfyllningsblock och pellets av bentonit enligt den återfyllningsdesign som föreslagits inom projektet ”KBP1003 System design of backfill” (Arvidsson et al. 2015). Efter färdig installation trycktes buffertblocket uppåt mot återfyllningen för att simulera en svällande buffert mot en torr återfyllning. De vertikala krafterna på stålplattan, förskjutningen av buffertblocket och uppkomna tryck mot bergytan i fem punkter ovanför hålet mättes under hela försöket.

Den totala förskjutningen uppåt hos buffertblocket var ca 150 mm. Det maximala trycket ca 1 800 kPa uppnåddes efter 75–80 mm förskjutning varefter trycket sjönk och ett konstant resttryck på 1 200–1 400 kPa uppmättes.

Bara två av de fem trycksensorerna placerade på bergytan ovanför deponeringshålet visade signifikant ökade tryck. I taket mitt ovanför deponeringshålet uppmättes ett maximalt tryck på ca 350 kPa. I det vänstra hörnet i övergången mellan tak och vägg i tunneln uppmättes som mest ca 300 kPa.

Trycken mellan återfyllningsblocken mättes med speciella indikatorer (plastfilmer) som registrerade det maximala trycket som filmerna blivit utsatta för. Dessa indikatorer placerades på 41 olika positioner. Resultaten från mätningarna var däremot ganska osäkra. Trycket varierade mycket mellan mätpunkterna och en förväntad reduktion i tryck med avståndet från hålet registrerades inte men det är oklart om dessa trender är verkliga.

Återfyllningsblocken nära det simulerade deponeringshålet undersöktes noga under brytningen. Återfyllningsblocken just ovanför hålet hade till stor del skjuvats av vid randen av buffertblocket. Blocken i de första tre lagren hade stora skador emedan i de ovanliggande fyra lagren hade spruckit i några olika riktningar. Blocken i de fyra översta lagren hade mycket små skador och tycktes mest ha förskjutits lite.

Återfyllningsblocken ovanför deponeringshålet hade en uppenbart bågformad utbredning på grund av de större vertikala rörelserna i centrum än i periferin. De yttersta blocken nära väggarna tycktes ha rört sig utåt mot väggarna.

Lasten från det simulerade deponeringshålet tycks inte ha spridits i sidled annat än i början på försöket innan maximal last uppnåtts. Istället har många av blocken skjuvats av. Detta är i överensstämmelse med mätningarna av trycket med plastfilmerna mellan blocken men inte med de låga tryck som mättes i taket. Det tycks vara stor skillnad i uppförande före och efter att blocken skjuvats sönder.

Den totala förskjutningen av buffertblocket på ungefär 150 mm har enligt försöksresultaten fördelats på följande sätt mellan de olika delarna:

- Det 70–90 mm tjocka pelletslagret på golvet har komprimerats ungefär 30 mm.
- Det 430 mm tjocka pelletslagret i taket mellan det övre återfyllningsblocket och bergytan har komprimerats ca 40 mm.
- Blockdelen har komprimerats ca 80 mm genom hoptryckning av spalter, elastisk kompression av blocken och rörelser i sidled.

Mätningar av enaxliga tryckhållfastheten och draghållfastheten hos återfyllningsblocken visar att hållfastheten är låg i jämförelse med andra mätningar, i huvudsak beroende på den låga densiteten och låga vattenkvoten hos blocken. Spridningen i resultat var också stor på grund av bl a stora granuler i bentoniten. Men medelvärdet på tryckhållfastheten var ca 1 600 kPa, vilket stämmer väl överens med det maximala trycket som mättes i fältförsöket innan många av blocken började spricka. En preliminär slutsats är att mothållet mot uppsvällning kan avsevärt förbättras om återfyllningsblocken görs med högre densitet, och därmed får högre tryckhållfasthet.

Contents

1 Background

One of the most important tasks for the backfill is to restrict upwards swelling of the buffer in deposition holes. If the buffer can swell upwards it will lose density and by that also important properties. A possible scenario that could lead to such expansion of the buffer could be where the water inflow into the deposition tunnel is very low but at the same time there is a water flow into a deposition hole. This means that the buffer in the deposition hole will hydrate quickly and try to swell resulting in a pressure build up pushing the dry backfill upwards. The backfill blocks will be piled according to a predefined pattern and it is predicted that there will be an improved distribution of the restricting load (i.e. it is not only the self-weight of the directly overlying backfill blocks that is restricting the movements but also adjacent interlocked blocks). The slots between the backfill blocks and the rock and also the region above the blocks are to be filled with bentonite pellets and the compression properties of this filling will also influence the ability of the backfill to resist heaving of the buffer.

The scenario with buffer swelling upwards against a dry backfill has been modeled but the results from this work depend in-part on properties that have not been confirmed through field or laboratory measurements. The parameters used in the modeling of the load distribution in the block stack, especially the compression properties of the block joints and how the blocks are moving relative each other needs to be verified. In order to get more knowledge regarding this issue, a full scale test (the Buffer Swelling Test, SKB project KBP1012) has been performed at Äspö HRL.

The purpose of the Buffer Swelling Test is thus to check and calibrate parameters and models used for modelling the mechanical response of a dry backfill on upwards swelling of a wet buffer. The most uncertain properties that will be investigated are the properties of the joints between the backfill blocks and the lateral spreading of the vertical stress.

2 Test description

2.1 General test description

The Buffer Swelling Test (BST) was done in Äspö HRL. It was a complement to a test of backfilling a tunnel with backfill blocks (large scale installation test within "System design of backfill" (Arvidsson et al. 2015). The main purpose of the test was to verify the technique developed for filling a tunnel with backfill blocks. A drawing showing an overview of the test design is provided in Figure 2-1. A "simulated deposition hole" with a depth of about 1.5 meter was excavated in the tunnel floor. A concrete tube with an inner diameter of 1 600 mm was placed in the hole. The slot between the tube and the rock was filled with concrete. Four hydraulic jacks were placed on the bottom of the hole. A steel plate with an outer diameter of 1.75 m was placed on the hydraulic jacks in order to evenly distribute the forces to the buffer block placed on the steel plate. The main reason for having a buffer block was to simulate the upper part of the deposition hole in realistic way. The tunnel above the simulated deposition hole was filled with backfill blocks and pellets according to the backfill design suggested in Arvidsson et al. (2015). The buffer block was then pushed upwards by the hydraulic jacks during the test, simulating the swelling buffer from a deposition hole towards the backfilled tunnel. This is of course a very extreme situation that probably cannot take place but considered in the safety analysis and thus needed to be investigated. The fast rate of displacement is neither realistic but the influence of time is not considered and not believed to have a very strong influence. Altogether the case is pessimistically considered. The tunnel was drained in order to keep the blocks and pellets free from water so that dry conditions were simulated.

A detailed drawing showing all main components of the BST is provided in Figure 2-2.

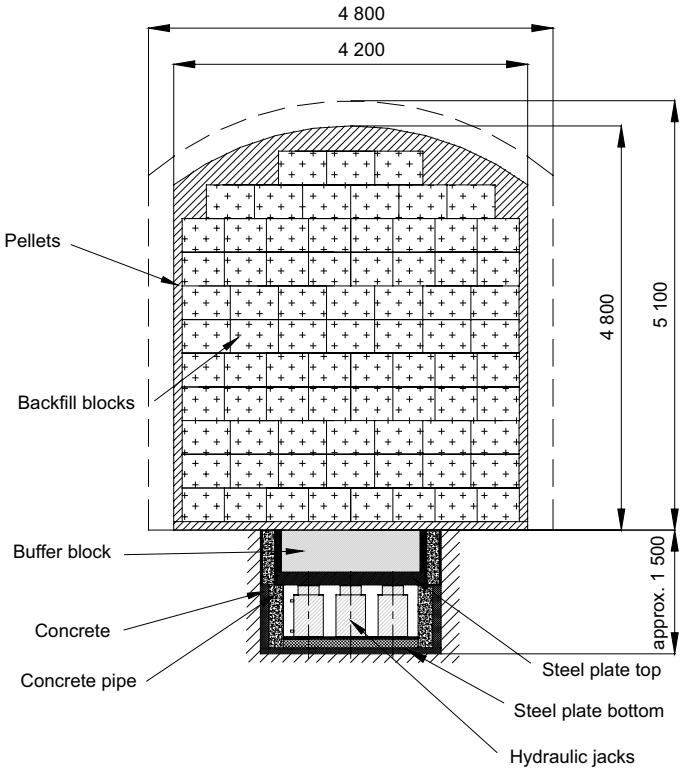

Figure 2-1. *Overview of the Buffer Swelling Test.*

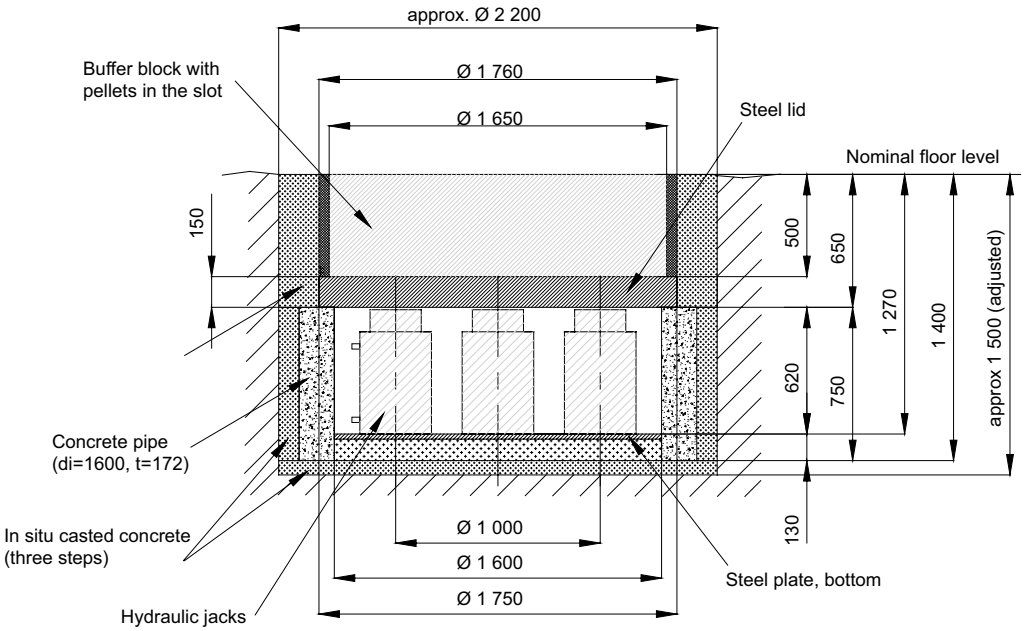

Figure 2-2. *Detailed description of the Buffer Swelling Test showing the main components of the test.*

2.2 Location

The BST test was performed in the TASS tunnel at Äspö HRL, located at a depth of about 420 m below ground (Figure 2-3).

In n the Swedish KBS-3 design adapted to the selected Forsmark site, the deposition holes are spaced to a distance of 6 meters. The installed backfill blocks in the BST extended a length of 12 meters. The simulated deposition hole was located at a distance of 6 meters from the tunnel end i.e. in the middle of the test length (Figure 2-4). This resulted in a backfill block installation that was completely consistent with an actual repository tunnel.

2.3 Measurements

2.3.1 Sensor description

During the conduct of BST a number of different measurements were made. A compilation of the instruments used is provided in Table 2-1. The test included both online measurements of pressure and displacements as well as measurements of the backfill blocks positions at the start of testing and after test termination.

Table 2-1. Instruments used in the test

Measurement	Number of transducers	Supplier	Model	Remark	Signal
Displacement	4	Solartron Amtele		320 mm Spring/Magnet	mA
Pressure block-rock	5	Geokon ÅF	4800	D=230 mm	Frequence
Hydraulic pressure	4	Druck Amtele	PTX 1400	Max 70 MPa	mA
Pressure between blocks	n/a	Caltech	Fuji LLW	Film	Optic

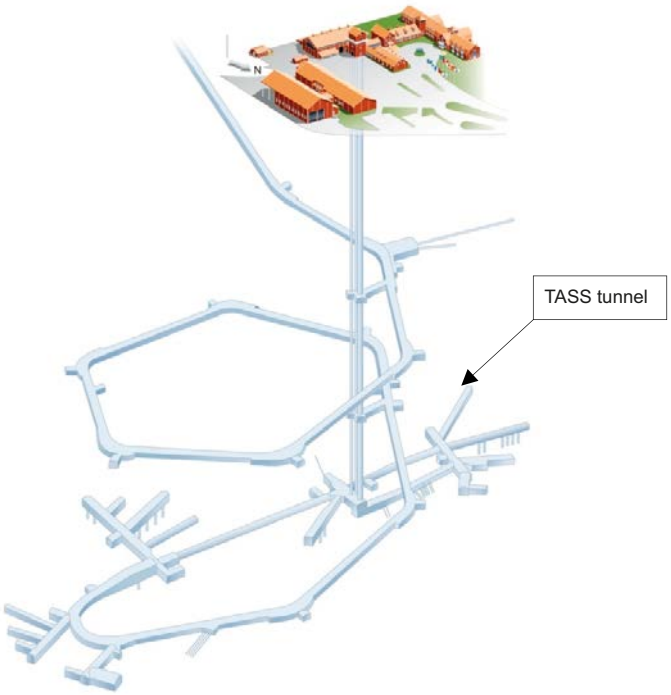

Figure 2-3. *Schematic drawing of the Äspö HRL tunnel system and the TASS tunnel position.*

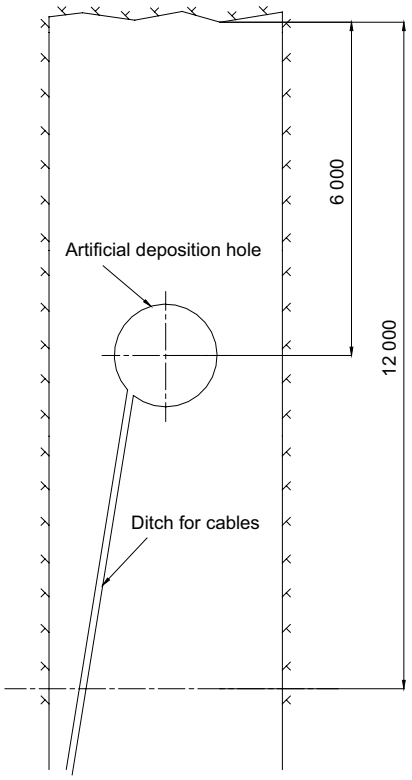

Figure 2-4. *Drawing showing the deposition hole position in the TASS tunnel.*

The measurements can be divided according to the following:

- **Simulated swelling pressure from the deposition hole**. The applied load from the hydraulic jacks on the steel lid was registered during the test. One pressure sensor was mounted on each of the hydraulic jacks. The total load acting on the steel lid can be converted to an average vertical stress simulating the swelling pressure from the bentonite in the deposition hole.
- **Displacement of the steel lid**. The displacement of the steel lid was registered by four sensors placed beneath the steel plate.
- **Pressure between the rock and the pellet filling**. Five pressure sensors were attached to the rock surface above the deposition hole in order to measure the pressure transferred from the backfill to the rock surface. A schematic drawing showing the positioning of the sensors is provided in Figure 2-5. Four of the sensors were placed in the ceiling and the wall in the tunnel section 6.0 m just above the deposition hole. In addition, one sensor was placed in the ceiling in the tunnel section 8.0 m at the top, about 2 meters away from the centre of the deposition hole. The exact positions of the sensors were after installation determined with a total station (a total station is an electronic theodolite (transit) integrated with an electronic distance meter (EDM) to read slope distances from the instrument to a particular point). The gaps between the backfill blocks and the rock was filled with pellets which means that the stress measurements were made at the pellets-rock surface interface. Modelling of the load distribution has shown that the pressure acting on the rock will be considerably lower than the pressure from the deposition hole since the load will be laterally spread in the block stack.
- **Pressure between blocks in the stack**. Contact sheets, approx. 0.1×0.1 m, consisting of thin plastic films (thickness approx. 0.2 to 0.3 mm) were placed between a large number of blocks located above the deposition hole. These sheets register the maximum pressure it has been exposed to through colour change.. The plastic film changes colour depending on pressure. Films with two different pressure ranges were placed at every position.
- **Block positions**. In order to trace the movements of the backfill blocks above the deposition hole during the test, a number of blocks were equipped with a reflector which made it possible to determine the exact position with a total station. After having finished the simulated buffer swelling, the steel lid was locked in its final position. During the excavation of the blocks, the position of the instrumented blocks was determined again. By comparing the block positions before and after the test, it was possible to get information regarding the distribution of the movements. Reflectors were placed on eighteen blocks above the deposition hole and at ten blocks at the backfill front.
- **Pellet slot widths**. In addition to the measurements described above, the slot widths between block stack and rock were determined at a large number of positions above the deposition hole. The same measurements were made again after the test during the excavation.

2.3.2 Data collection

The data collection was made with two different systems:

1. *Labview.* Pressure sensors and displacement sensors were logged with this system. The log interval was set to every third second during the first five hours (during the load steps) and was then changed to every fifth minute.
2. *Geokon*. Pressure sensors on the rock surface were logged with this system. The logging interval was set to every thirty seconds.

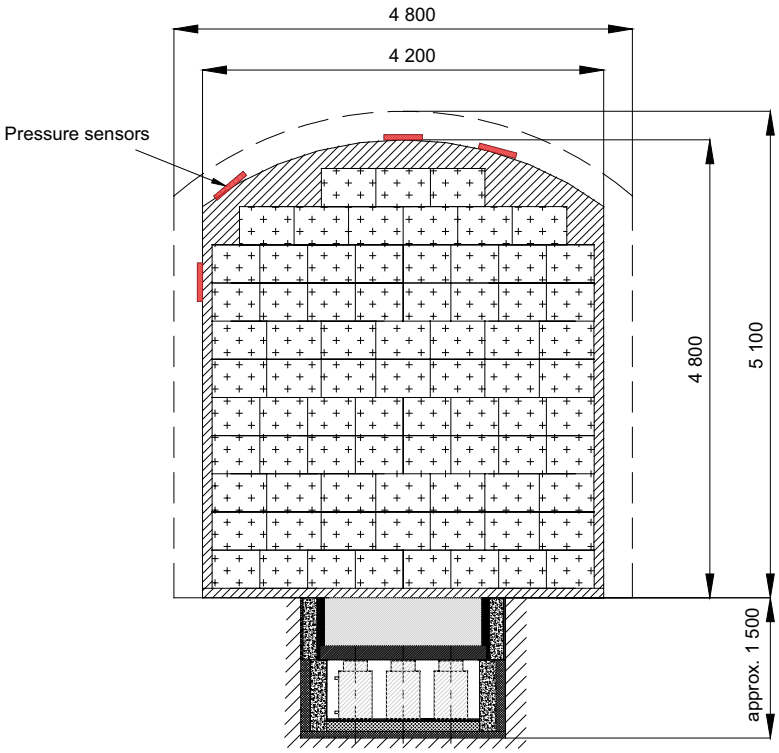

Figure 2-5. *Schematic drawing showing the positions of the pressure sensors on the rock surface.*

3 Installation

3.1 General

The artificial deposition hole was made according to the plans shown in Figure 2-2. It was important to ensure that the top of the buffer block was at the same level as the nominal tunnel floor.

3.2 Installation of equipment in deposition hole

The four hydraulic jacks were located in the deposition hole with the centre points on a circle with a diameter of 1.0 m, Figure 3-1. The angular distance between the jacks was 90°.

The displacement sensors were placed between the jacks. The sensors were locked to a stand which was bolted to the bottom steel plate. In order to secure the contact between the sensor top and the upper steel lid, the sensors were spring loaded and in addition magnets were mounted at the top to further ensure that the contact between the displacement sensors and the top lid was maintained.

After construction of the artificial deposition hole and the ditch for the cables, it was noted that there was a detectable water inflow from the cable ditch into the hole (see dark areas in Figure 3-1. In order to prevent continuing water filling of the hole after closure, a small water collection vessel was bolted on the hole wall just beneath the cable ditch, Figure 3-2. A tube connected to a pump was placed in the vessel and all water flowing to the vessel was collected and removed. After having finished the installation of jacks and sensors, the upper steel lid was installed, Figure 3-3.

Figure 3-1. *The four hydraulic jacks and the four displacement sensors installed in the artificial deposition hole*

Figure 3-2. *Close-up showing the entrance leading out cables from the deposition hole. Note the vessel that collects water leaking in from the cable ditch. A tube, connected to a pump, was continuously leading out water from the vessel.*

Figure 3-3. *Installation of the steel lid covering the hydraulic jacks.*

3.3 Test run of the hydraulic equipment

After having installed the steel lid, the tubes from the jacks were connected to the hydraulic pump. In order to check that the equipment and sensors were working, a number of tests were done where the jacks below the lid was pressured and upwards displacements at different rates were accomplished.

3.4 Installation of buffer block

The buffer block was installed by use of a vacuum lift specially designed for this purpose, Figure 3-4. The buffer block had a water content of 17 % and a bulk density of 2 070 kg/m^3. The block was originally manufactured as a spare block for the Multi Purpose Test, which is a full scale in situ test of KBS-3H.

3.5 Installation of sensors on the rock surface

The five Geokon pressure cells were installed on the rock surface at the crown of the tunnel before any other installation work started, Figure 3-5. At the desired positions for sensor installation, the rock surface was evened out with cement in order to achieve a suitable surface for the sensors. The sensor plates were then bolted to the rock surface.

After installation of the sensors, a handheld instrument was used in order to get a zero reading of the sensors. This value was later used for the data evaluation.

The measured distance from the uppermost backfill block surface to pressure sensor 1 was 427 mm (subsequently filled with pellets).

Figure 3-4. *Installation of a buffer block on top of the steel lid.*

3.6 Installation of pressure indicators

Pressure indicators were placed at 41 positions in total; five positions on the buffer block's upper surface and 36 positions in the block stack. At every position, two sensor films with different measuring ranges were placed (0.5–2.5 MPa and 2.5–10 MPa), Figure 3-6 and Figure 3-7. The positions of the indicator strips in the block stack are shown in Figure 3-10. Details regarding the pressure indicators and their calibration are provided in Chapter 5.

Figure 3-5. *Five pressure sensors were installed in the ceiling above the deposition hole.*

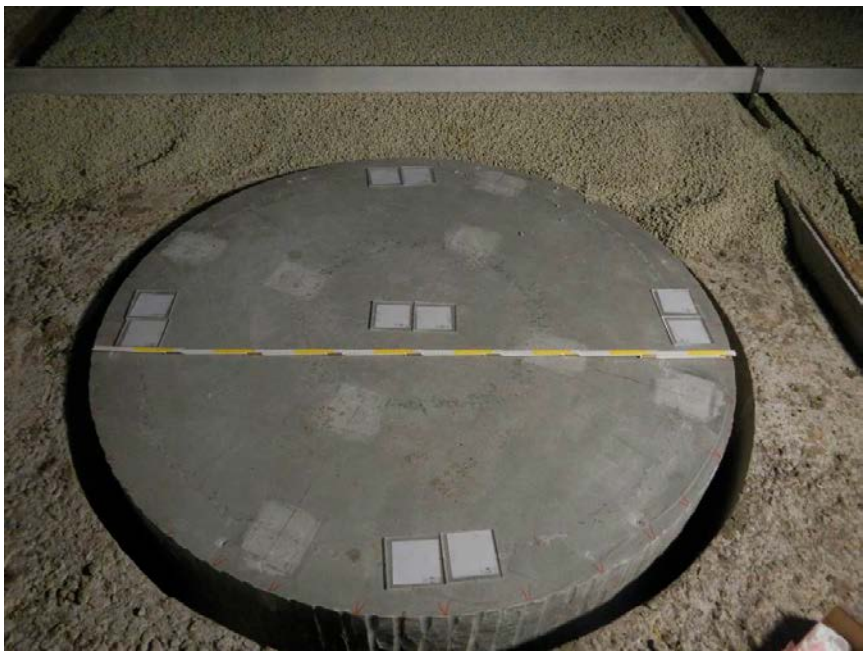

Figure 3-6. *Pressure indicators placed on the buffer block.*

3.7 Measurement of block positions

18 blocks located above the deposition hole were equipped with a reflector and thereafter the positions were determined with a total station. In addition, ten blocks were instrumented at the backfill front after having finished the block installation (Figure 3-8 to 3-10). The block positions were determined again in conjunction with the test termination.

The height of the block stack was measured to 4425 mm (11 blocks with a nominal height of 400 mm gives 4400 mm). This suggests that the average horizontal joint thickness between each backfill block is 2.5 mm. The nominal width of the block stack at the base is 4000 mm (the actual width was not measured).

Figure 3-7. *The pressure indicators were placed between the backfill blocks at selected positions. Two sensors with different measuring range were placed on each block.*

Figure 3-8. *The block positions were determined with reflectors at ten points at the end of the block stack.*

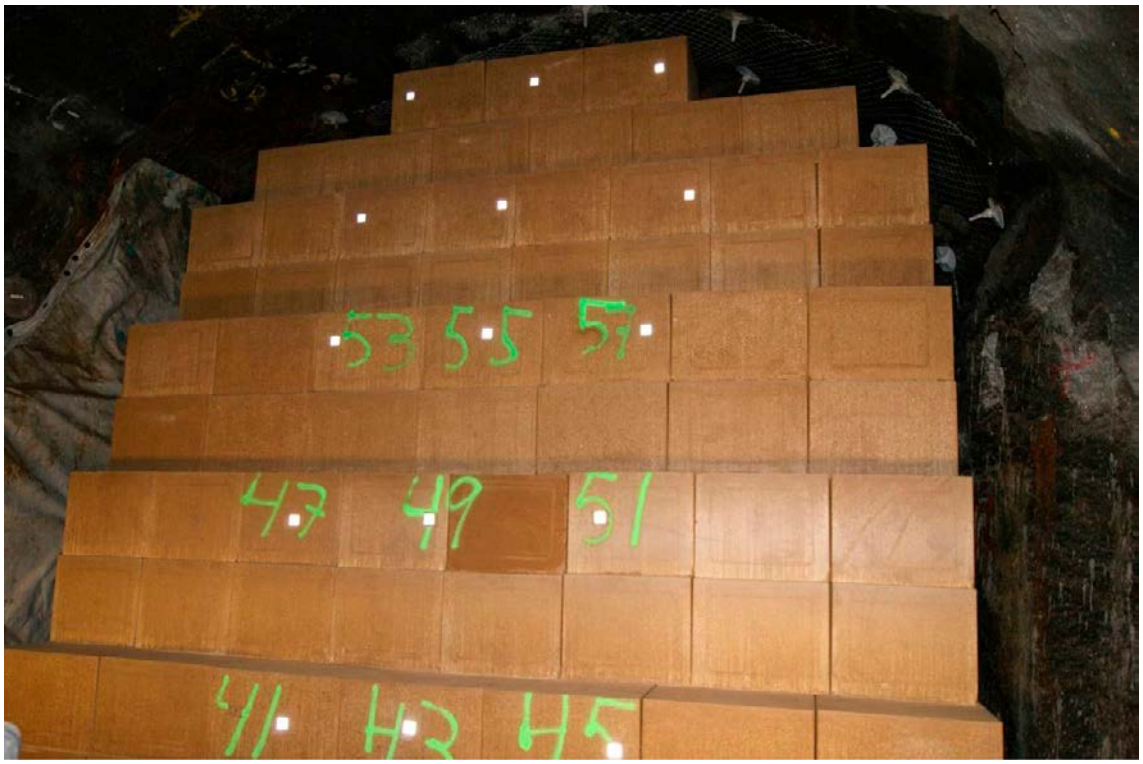

Figure 3-9. *The block position were determined with reflectors at eighteen points at the inclined vertical layer 4 just above the deposition hole.*

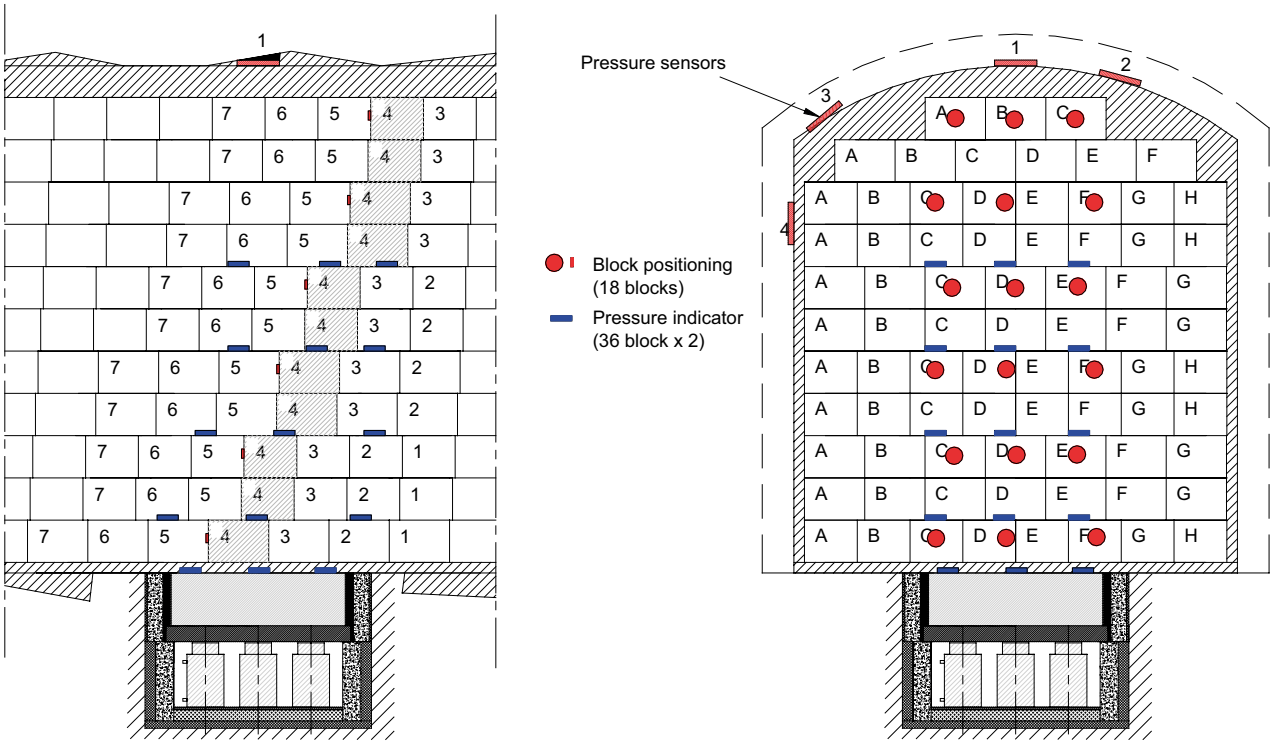

Figure 3-10. *Schematic drawing of the block positions above the deposition hole. The pressure indicators (blue) were placed both at the top of the buffer block and between the blocks in the stack above. The position of eighteen blocks in the vertical inclined layer 4 (red dots) were determined using a total station.*

3.8 Measurement of pellet slot widths above the deposition hole

The distances between the block stack and the rock surface were measured at a large number of positions for the vertical block layer 4 above the deposition hole, see description of the block layers in Figure 3-10. The measured distances are presented in Figure 3-11.

3.9 Installation of bentonite pellets

Pellets were blown into the remaining gaps between backfill blocks and rock walls. The installation was made using a standard shotcrete equipment. The outermost part of the pellet filling was pre-wetted, in order to keep loose dry pellet materials from falling out of the downstream face. The average dry density of the pellet filling was calculated to 940 kg/m^3 (Arvidsson et al. 2015).

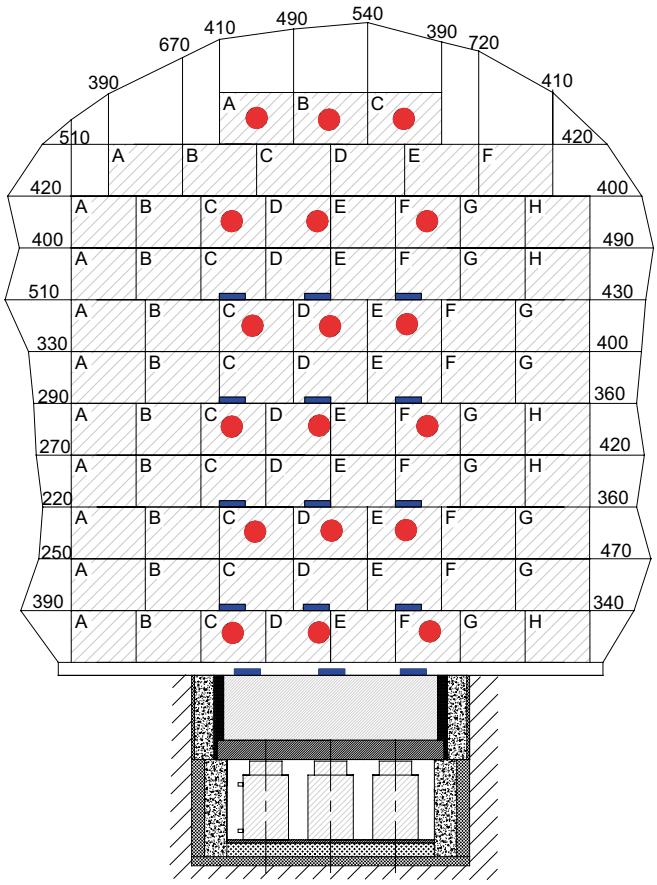

Figure 3-11. *Schematic drawing showing the measured distances between the blocks and the rock surface for the vertical block layer 4 above the deposition hole.*

4 Results

4.1 General

One result of the pre-tests with the hydraulic equipment was that it would be difficult to apply a constant rate of displacement that was low enough to simulate a buffer-backfill interaction. It was therefore decided to instead apply the load in steps with a certain relaxation time (15 minutes) between each step.

The load steps were made by moving the steel plate upwards either 5 or 10 mm (approximately).

4.2 Data registered during test

4.2.1 Applied pressure and displacement

Figure 4-1 shows the registered oil pressure in the four hydraulic jacks plotted versus time. It was noted that there were differences in pressure between the four jacks during the pressure increase and also that the highest or lowest pressure shifted between them. After having finished a pressure increase step, there was still a remaining difference in pressure between the jacks.

During the relaxation period following a pressure increment there was a small decrease in hydraulic pressure in the jacks which probably resulted from small movements in the block stack, allowing decrease of load on the plate-buffer contact. Detailed plots of the load-decrement data are provided in Appendix 2.

The oil pressure in the jacks provided in Figure 4-1 can be recalculated to force. The sum of the loads and thus total force on the steel plate is plotted in Figure 4-2.

Figure 4-3 shows the registered displacement of the steel lid plotted versus time. The differences between the four sensors were very small during the whole test duration. After having finished the period of increased load the displacement was zero.

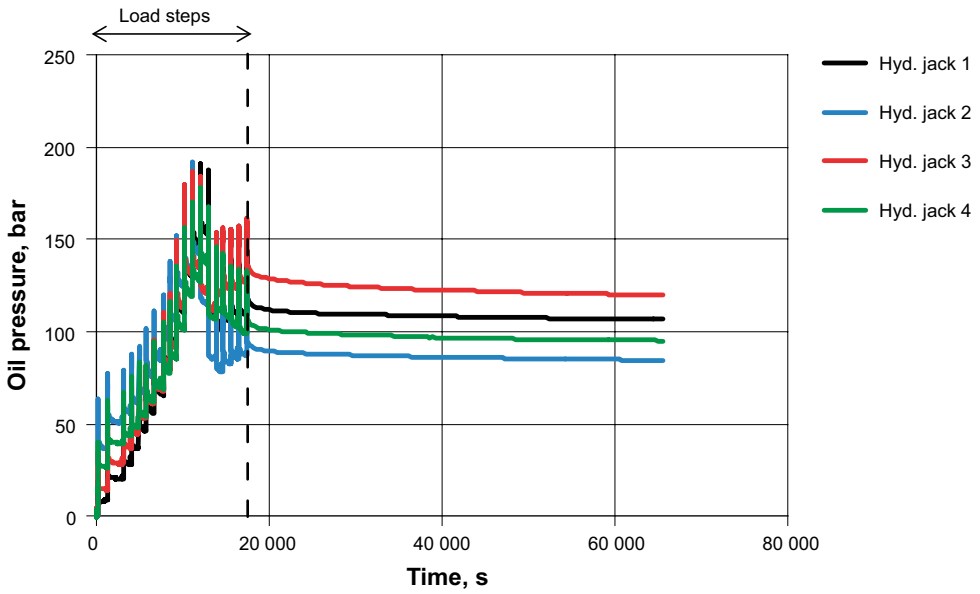

Figure 4-1. *Registered oil pressure in the four hydraulic jacks plotted versus time.*

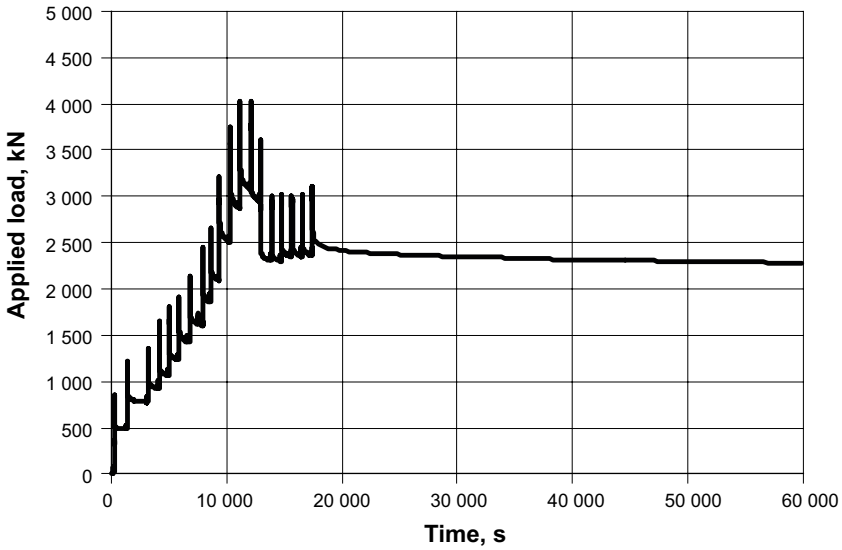

Figure 4-2. *Applied total load from the hydraulic jacks plotted versus time.*

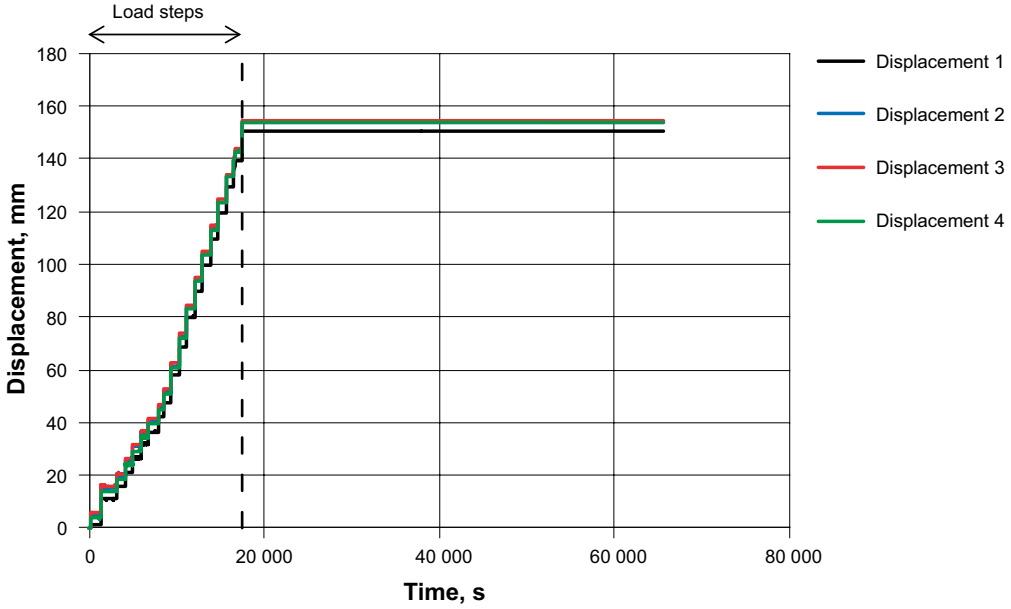

Figure 4-3. *Registered displacement of the steel lid plotted versus time.*

The total load shown in Figure 4-2 can be re-calculated to vertical stress acting on the cross section area of the buffer block by dividing the force with the area of the block, which would correspond to the simulated swelling pressure. Figure 4-4 shows the vertical pressure plotted versus the displacement of the steel lid. The maximum stress occurred after approximately 80 mm displacement. After this time, inducing a continued displacement resulted in a constant (but lower) residual or post-failure stress. After inducing more than 150 mm of vertical displacement the test was terminated.

4.2.2 Pressure measurements against rock ceiling and walls

The results of the pressure measurements at the rock surface above the deposition hole are presented in Figure 4-5. Significant pressures were only registered by sensor 1 (immediately above the deposition hole) and by sensor 3 (at the corner between the ceiling and the wall), the locations of these sensors are provided in Figure 3-10

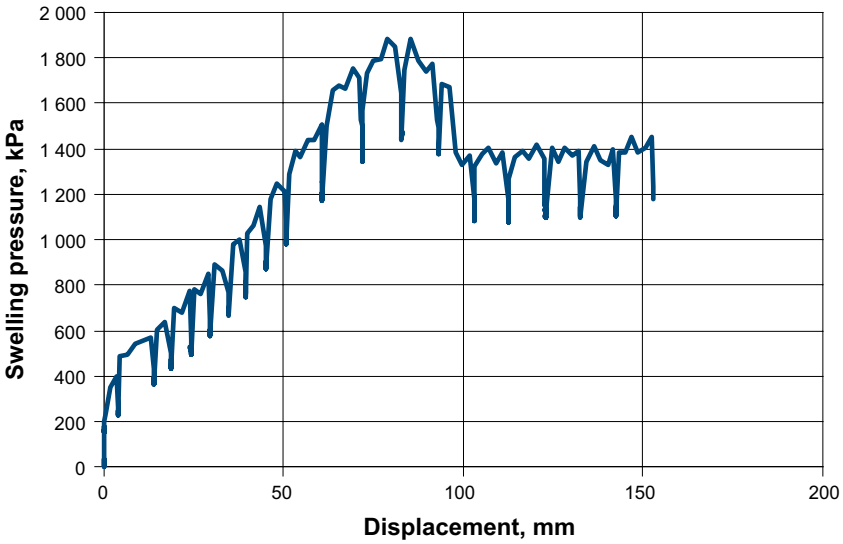

Figure 4-4. *Total average vertical stress from the buffer block plotted as function of the displacement.*

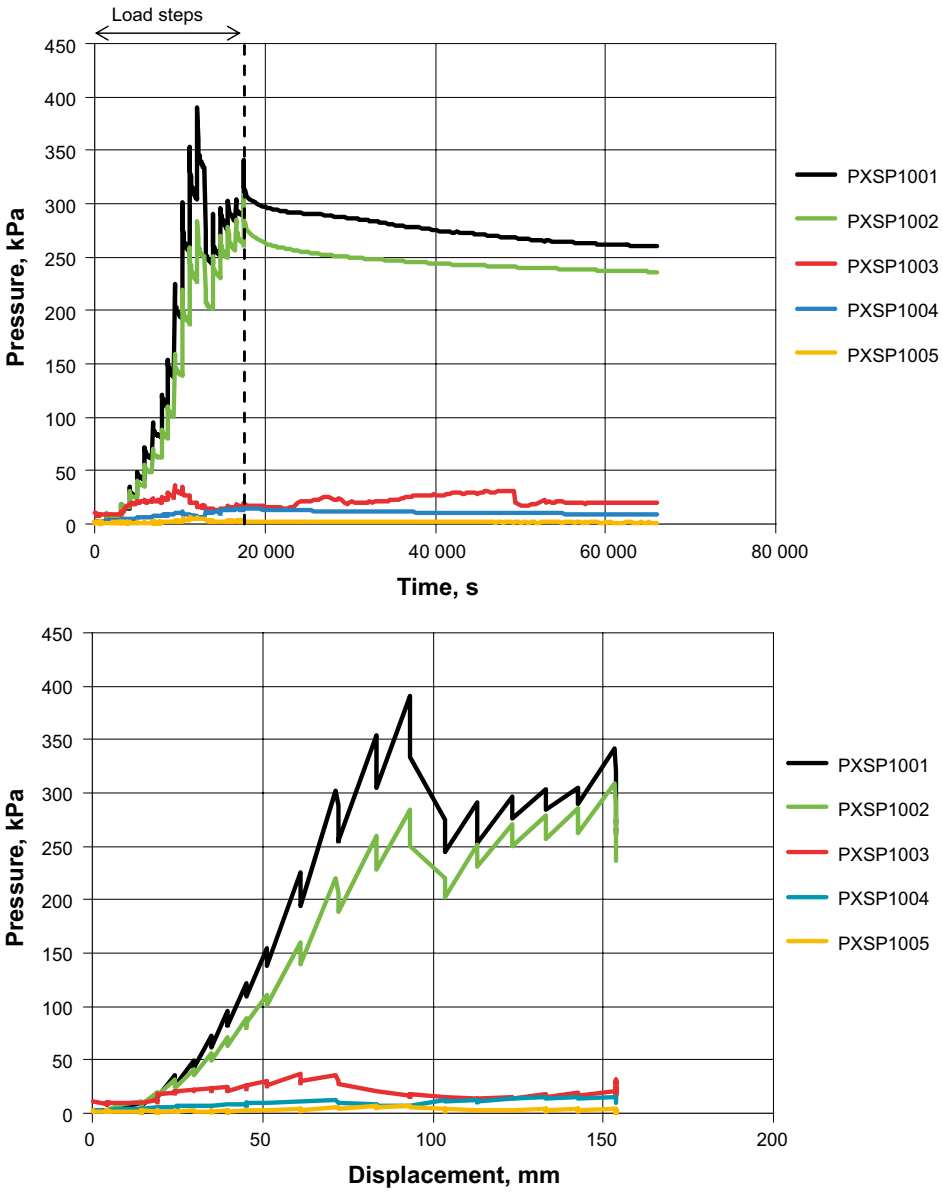

Figure 4-5. *Upper: Pressure registered at the sensors placed on the rock ceiling and walls plotted versus time. Lower: Pressure registered at the sensors placed on the rock ceiling and walls plotted versus displacement.*

4.2.3 Pressure measurements between blocks

The results and the evaluation of the pressure film measurements are described in Chapter 5.

4.2.4 Visual observations during test

In the final part of the test, it was observed that the pellet filling at the ceiling had moved forward about 40 to 50 mm, Figure 4-6. During the last load step the location of the outer edge of this material was observed very carefully but it was not possible to detect any movement during this time.

4.3 Excavation

4.3.1 General

The excavation of material from the BST was mainly done using a telescopic forklift. The blocks were pulled down, one by one, into the space in front of them and when there were sufficient materials in front of the still-standing portion of the block stack, these were lifted out from the tunnel to a waiting truck. A couple of hundred blocks were saved and these were lifted carefully down to pallets by using a vacuum tool attached to the lift.

4.3.2 Block movements

Measurement with the total station

A description of the installation and location of the reflectors is provided in Section 3.1.7 and in Figures 3-8, 3-9 and 3-10. The results from the measurements are provided in Appendix 1.

The results from the measurements showed that the movements at the front of the backfill block stack were very small, about 2–3 mm upwards (vertical) as a maximum. The movement of blocks above the deposition hole were, however, large, see Figure 4-7. The uppermost blocks had moved upwards approximately 36–38 mm while the blocks closest to (over) the deposition hole had moved upwards by135 mm at the most.

Figure 4-6. *The pellet filling on top of the block stack had been pushed out about 40 to 50 mm. The outermost part of the pellet filling was pre-wetted, during the BST construction in order to keep loose dry pellet materials from falling out of the downstream face. The result of this is that the pellets stick to the ceiling and when extruded by internal deformation, do so as a plastic mass.*

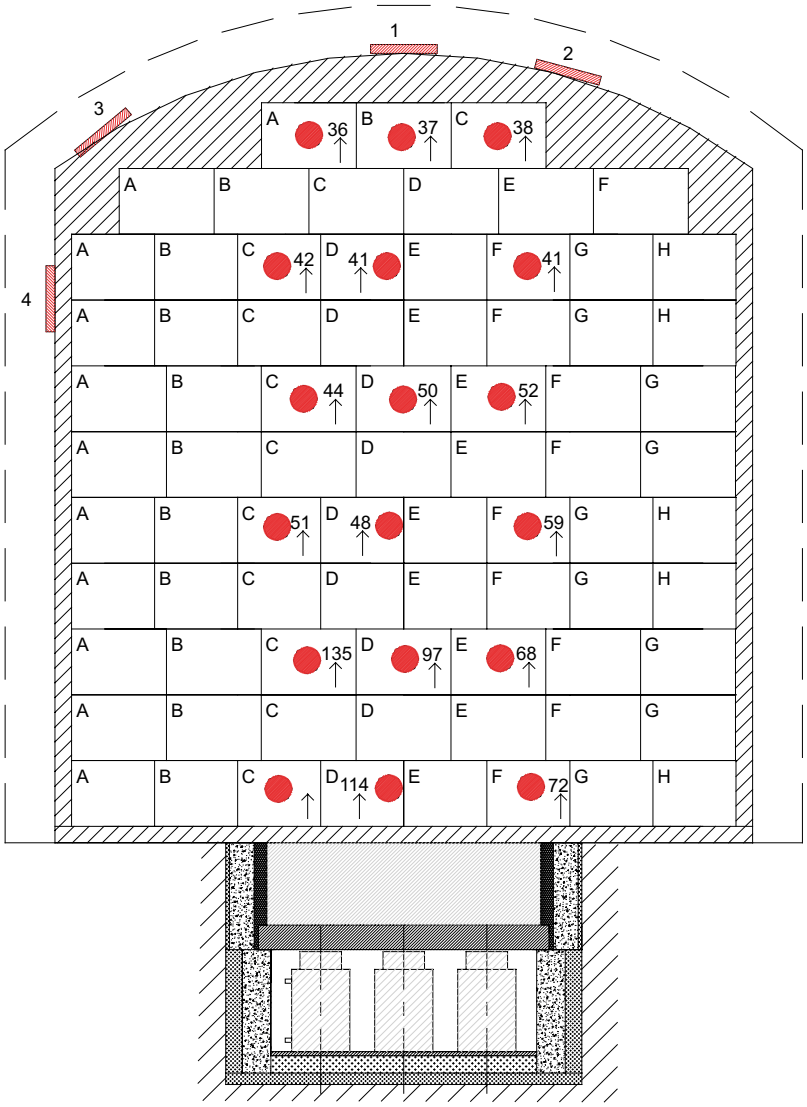

Figure 4-7. *Vertical layer 4 immediately above the deposition hole showing block locations measured with a total station before and after installation. The numbers beside each red point indicate the vertical movement of each block.*

Visual inspection

The buffer block was displaced upwards by approx. 150 mm. This movement resulted in a compaction of the pellet floor layer between buffer block and backfill block and a concurrent displacement of the adjacent backfill blocks.

The photo provided as Figure 4-8, shows the block stack at vertical section 6 (see Figure 3-10), which goes over the deposition hole at the top. Cracks can be seen in some of the blocks (e.g. block marked 77 and the one immediately below, see black arrow in photo) but many of the blocks in the stack have displaced laterally towards the right rock wall.

This section includes many photos and in the end some comments and conclusions. Only a preliminary evaluation has been done in the final chapter of this report. More detailed evaluation is done in the two modelling reports. The lateral movements of blocks are suggested to be caused by the spreading and reduction of the vertical stress with distance from the buffer. This spreading requires a lateral stress that will contribute to a lateral displacement.

Figure 4-8. *The block stack at the vertical section 6 (see Figure 3-10) just before reaching the deposition hole (at the lower part) and close to the midpoint over the deposition hole at the top of the block stack.*

Figure 4-9. *Photo showing the block stack top and the pressure sensor on the rock ceiling just above the deposition hole (black arrow).*

Figure 4-10. *The pressure indicator on the photo was positioned on top of layer 3. The block below has been sheared and the shear surface can be seen very evidently (black arrow). Parts of the block have been vertically sheared approx. 50–60 mm relative the rest of the block.*

Figure 4-11. *Some additional blocks of the ones shown in Figure 4-10 have been removed and the shear surfaces can be seen clearly (black arrow at the top on block layer 3).*

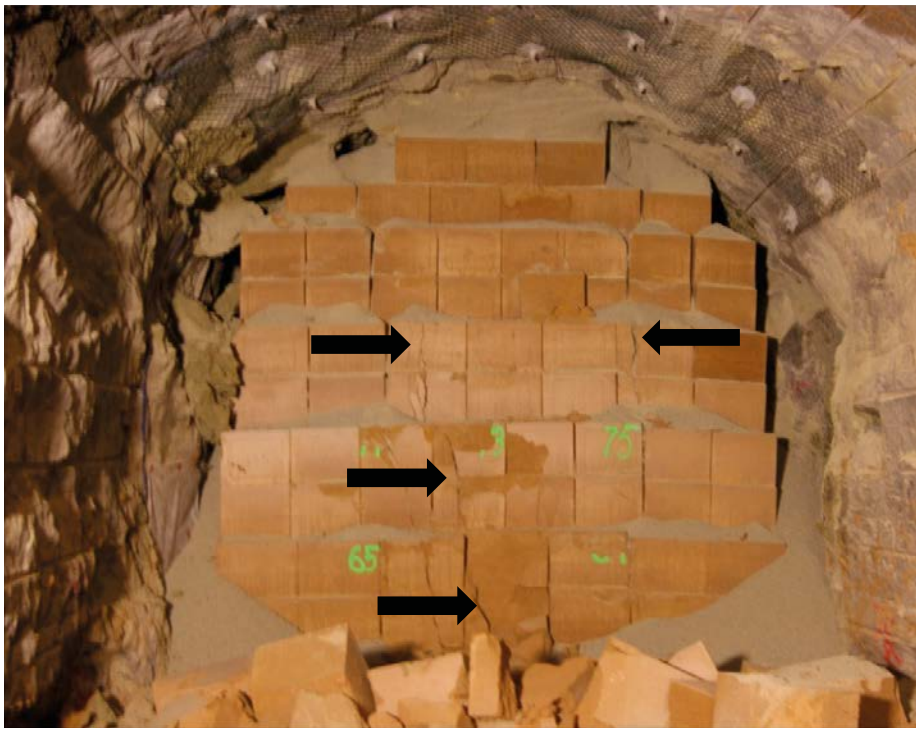

Figure 4-12. *Overview showing the shear zones in vertical layer 5 (see Figure 3-10). The cracking is severe on the left side but also evident on the right (black arrows).*

Figure 4-13. *The vertical layer 4 (see Figure 3-10) above the deposition hole, where blocks were equipped with reflectors and their position determined with a total station before and after test.*

Figure 4-14. *The edge of the buffer block (black arrow) and the sheared block above.*

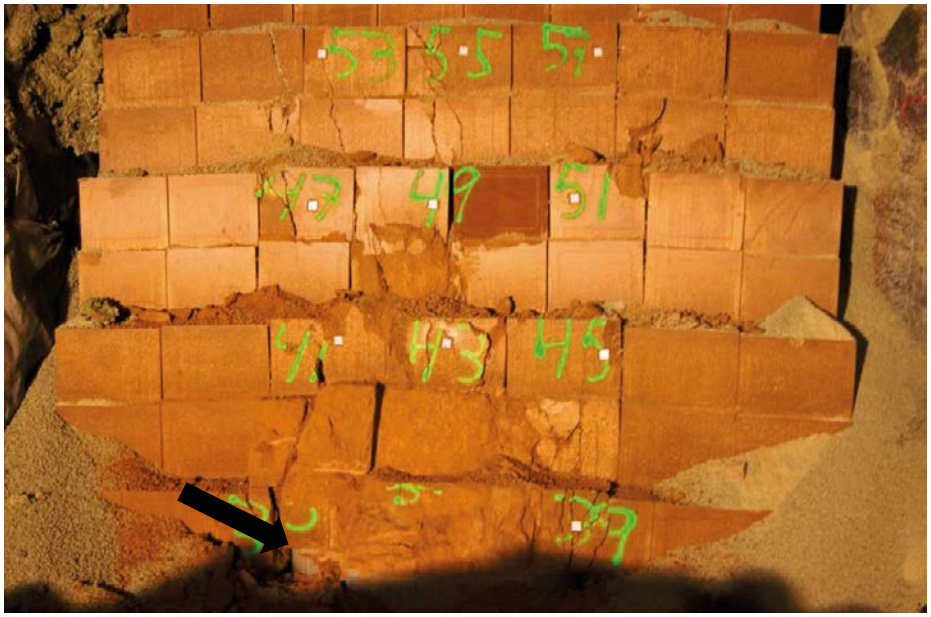

Figure 4-15. *The shear surface just above the front of the buffer block (black arrow) can be seen very clearly together with fractures extending vertically upwards and to the left.*

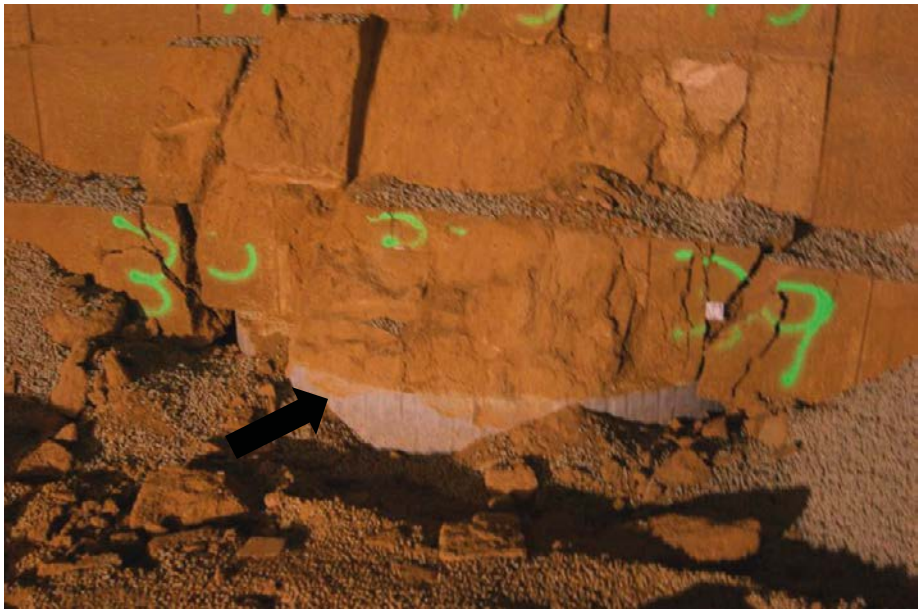

Figure 4-16. *Close up of the buffer block at the front (black arrow), showing extensive near-vertical fracturing of backfill blocks near outer edges of buffer.*

Figure 4-17. *Overview of the block stack above the deposition hole with buffer showing at the base (black arrow). The shearing of backfill blocks is mostly to the left of center, while blocks on the right side seems to have moved out into the pellet slot rather than failing.*

Figure 4-18. *Extensive shear surfaces and fractures in the blocks immediately above the deposition hole.*

Figure 4-19. *Shear surfaces on vertical block layer 3. See also Figure 4-11.*

Figure 4-20. *Photo showing the buffer block surface, the pellet layer and the backfill blocks at the midpoint of the deposition hole.*

Figure 4-21. *The backfill at the innermost part of the deposition hole in vertical layer 2 (see Figure 3-10). The shear and fracture surfaces can be seen very clearly.*

Figure 4-22. *The block stacks inside the deposition hole beyond vertical section 1 are almost unaffected by the buffer heaving.*

Figure 4-23. *The buffer block is uncovered.*

Figure 4-24. *The buffer block is rather unaffected by compressive interaction with backfill blocks, only a few fractures can be seen.*

4.3.3 Pellet slot widths

Pellet layer above buffer block

The pellet layer between the buffer block and the backfill blocks above had an initial thickness of between 70 and 90 mm. The layer was thinnest at the front and thicker at the innermost part. The difference depends mainly on the tunnel inclination.

The thickness of the pellet layer was measured during the excavation. It was found that the thickness at the end of the test was about 25 mm at the front and approx. 45–50 mm at the midpoint of the buffer block Figure 4-25 and Figure 4-26.

Pellet-filled slots between the backfill blocks and the rock

The widths of the slots that were filled with pellets were measured around the block stack for a vertical section (the same profile as was equipped with reflectors(see Figure 3-10)). A new set of measurements was made during the excavation of the BST. The results are presented in Figure 4-8. The determined values show that change in gap profile was not uniform or consistent in pattern, varying considerably locally. The displacement data do clearly show that the block stack has been moved upwards about 30 to 70 mm. The distance between the pressure sensor positioned at the ceiling (sensor 1, Figure 3-10) and the rock stack was determined during the installation and again during the excavation. The difference between the two measurements showed that the block stack had moved upwards approx. 44 mm.

Pellet layer at ceiling

The distance between backfill block stack and pressure sensor on the rock surface right above the deposition hole, was during installation measured to be 427 mm. Corresponding measurement was made during the excavation and the distance after the test was found to be 383 mm, Figure 4-11. This means that the block stack had moved approx. 440 mm upwards. The measurement of the block positions made by total station and reflectors, see section 4.3.2, indicated that the uppermost blocks had moved between 36 to 38 mm upwards.

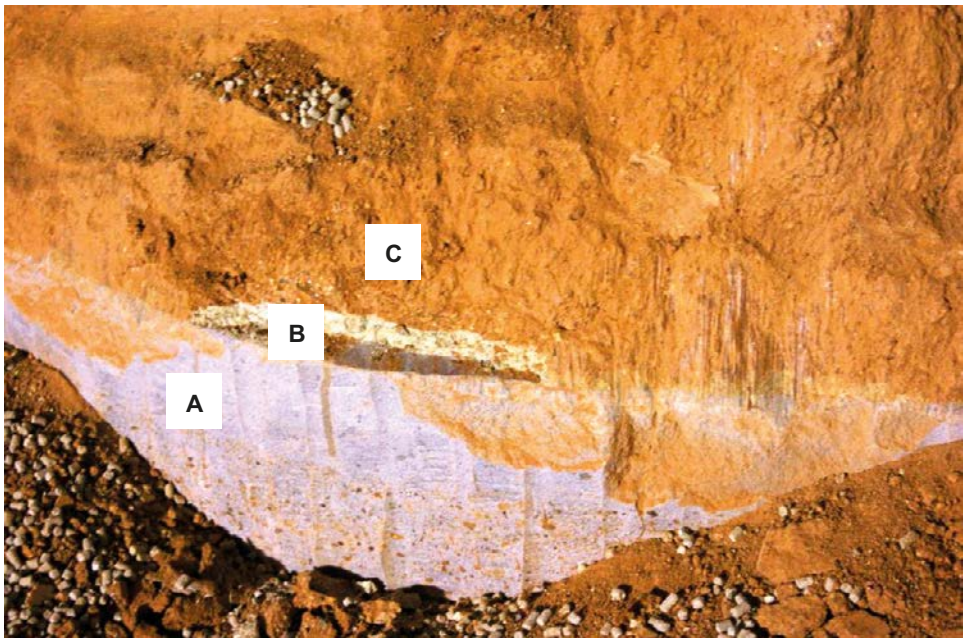

Figure 4-25. *Photo showing the upper part of the buffer block (A), the compressed pellet layer (B) and the sheared backfill blocks above (C).*

Figure 4-26. *Photo showing the middle part of the buffer block together with the compressed pellet and backfill blocks (same as Figure 4-20).*

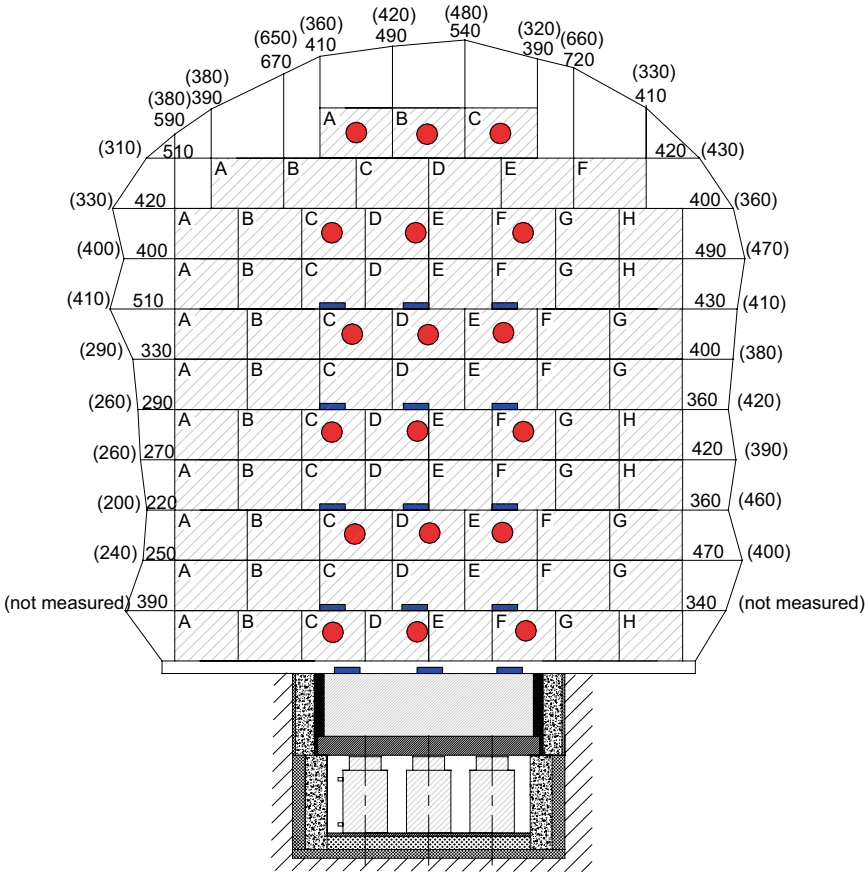

Figure 4-27. *The measured slot widths and gap at crown of tunnel between the block stack and the rock surface before and after the test. These volumes were filled with bentonite pellets. The values shown in brackets were determined during the excavation i.e. after the vertical movement of the buffer block had ended.*

Figure 4-28. *The distance between block stack and the pressure sensor (1) was determined to be 383 mm after test. .*

4.4 Compression properties of the pellet fillings

The most important property of the backfill for the displacement of the buffer block is (beside the compression strength of the blocks and the compression properties of the joints) the compression properties of pellet fillings. These have been investigated in a subproject within the System Design of Backfill (Andersson and Sandén 2012).

Figure 4-29 shows results of a number of compression tests made in a large oedometer (Andersson and Sandén 2012). The strain of several different pellet fill options are plotted versus applied stress. In the Buffer Swelling Test, the maximum applied pressure from the buffer block was approx. 1.8 MPa. Figure 4-29 shows that this pressure corresponds to a strain of approx. 27–30 %. The measured compression of the layer above the buffer block was approx. 30 to 37 %, which is a little higher than observed in the laboratory. The comparison of lab and field data should also recognize that the buffer block was pushed an additional 80 mm upwards after reaching the maximum vertical stress. This reflects pellets (and backfill blocks) that were no longer consolidating but crushing. The BST arrangement also allowed for internal (and external) movements and volume strains as well as lateral displacement to occur, whereas the laboratory pellet tests did not allow for such mechanisms, hence larger strains could be reasonably expected to be observed in the field test.

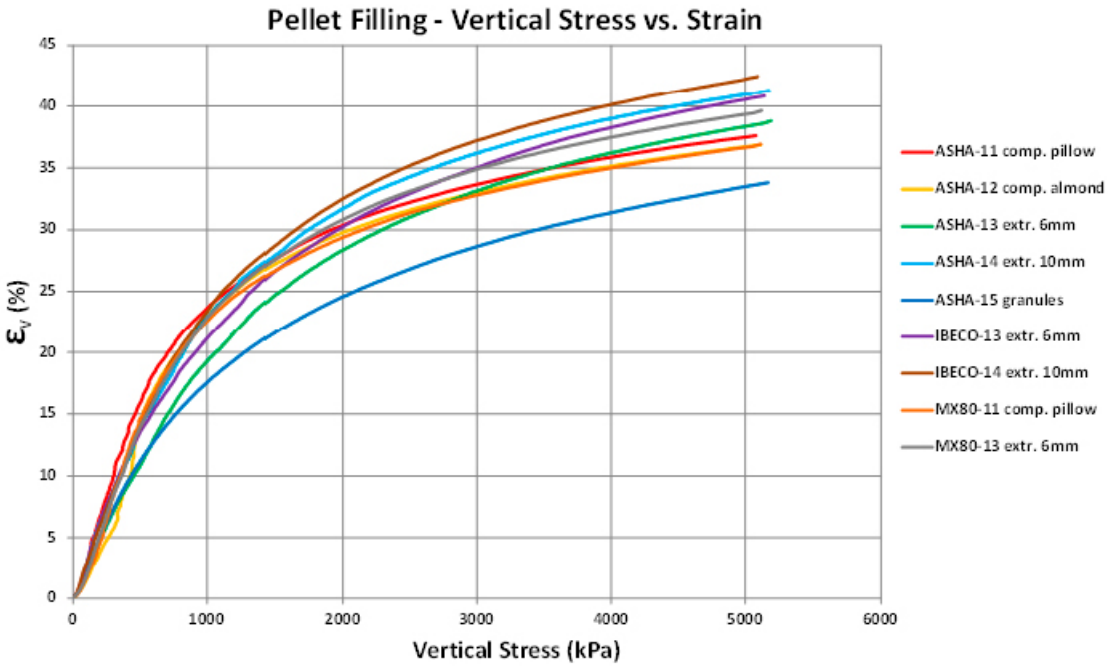

Figure 4-29. *The strain of different pellet fillings plotted versus stress (Andersson and Sandén 2012).*

5 Pressure measurement with pressure indicators

5.1 Background

In order to investigate the pressure distribution in the stacked blocks in the backfill a number of sheets of pressure sensitive film were placed between blocks. The pressure film consists of two thin films that react to pressure through microbubbles filled with ink that burst at a specific pressure, see Figure 5-1. The color intensity and distribution of the color on the film is therefore a representation of the maximum pressure the film has been subjected to. The advantage of this technique is that no power or signal cables are needed. The disadvantage is that only the max pressure is registered. In addition the use of this technique was previously untested and the accuracy very uncertain.

5.2 Installation

Two sets of pressure films were used, one with the pressure range 0.5–2.5 MPa and one with the pressure range 2.5–10 MPa. They were always placed together in the experiment in order to cover a large variation in pressure. A sticker with a serial number was used to identify the films. The idea was to place films on top of the buffer block and in-between the backfill blocks in the stack. They were placed on top of layer 1, 3, 5 and 7 and on the buffer block as shown in Figure 3-10 and 3-11. The pressure films were placed after pausing the stacking by the robot. Due to the programmed stacking procedure it was not always possible to place the film exactly at the intended location, but the general placement was in fair agreement with the plan. Altogether pressure films were installed at 41 locations, each with two films per location.

5.3 Retrieval

When the test was dismantled the pressure films were collected. All films were retrieved, although one was ripped in two pieces and two lost their sticker. Their identity could be established since their location was known and the remaining films had identity stickers attached. Each pressure film was scanned to an image file and plotted as shown in Figure 5-2. Finally the scan was analyzed according to Section 5.4.

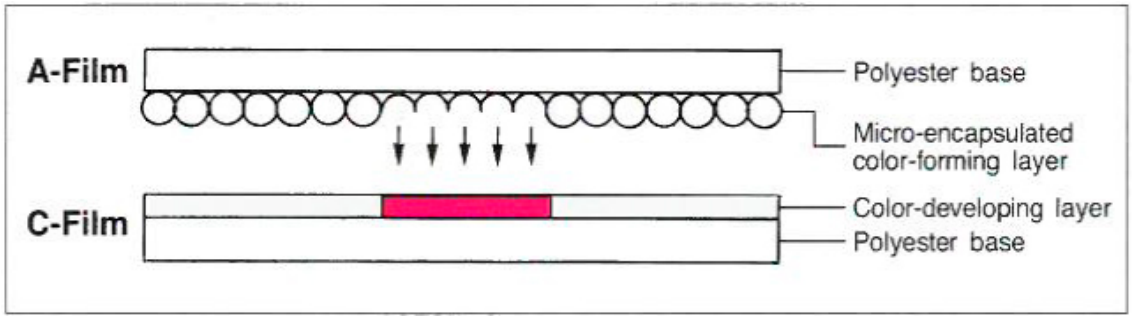

Figure 5-1. *Description and function of the pressure film. Taken from the manufacturer's datasheet.*

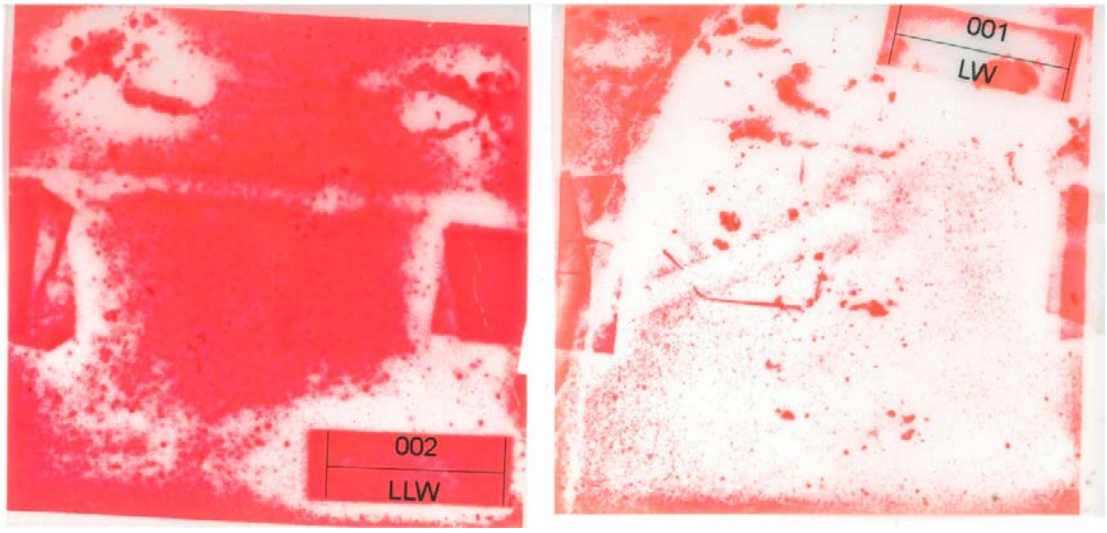

Figure 5-2. *Pictures plotted from the scanning of two pressure films. The effect of the sticker tape holding the sheets together is seen at the left and right sides.*

5.4 Evaluation

The pressure films were analyzed by an image program (ImageJ) that could present a histogram of the intensity in the scanned film, see Figure 5-3. The outer rims of the films and the tapes were discarded since those parts were judged to have been affected by the handling. Ideally the result should be either a burst microbubble (red) or not (white) but the resolution was not high enough so each pixel represents a number of microbubbles that were either unaffected or had burst. The colors were converted to greyscale and the resulting histogram was a representation of the number of pixels at different grades of grey. When evaluating the results all white pixels were discarded and the rest were compared to the total number of pixels in a scan. This is not a very accurate evaluation but had previously been tested in the laboratory and found to be the best evaluation method. Since the two films had different range, both had to be analyzed and the results compared with the film. The pressure was then evaluated as the number of non-white pixels divided to the total number of pixels multiplied with the maximum pressure of the film (2.5 MPa or 10 MPa). The films were also checked visually. The result was rounded to the nearest 0.5 MPa.

A laboratory test with the purpose of investigating the effect of time, i.e. if prolonged exposure would alter the result, was made by placing a large weight on a film for a week and then comparing it with a film that was only loaded for 1 minute. The result after one week was 35 % higher stress than after one minute when evaluated as described.

Since the exposure in the tunnel and the time between pressure and the subsequent reading can affect the result of the pressure, a normalization of the results was made. The measured maximum pressure at the base of the buffer block was 2 MPa according to the reading of the hydraulic pressure in the rams lifting the buffer block. The average value of the 5 sets of two pressure films placed on top of the buffer block was 4.3 MPa if evaluated according to the technique described. A normalization factor of 0.465 was therefore used on all readings to compensate for this.

5.5 Results

Both the variation in color in the pressure films and the variation in evaluated histogram showed that the variation in pressure on a film is large, mainly due to uneven block surfaces and uneven heights of the blocks yielding an irregular stack.

The results of the evaluated pressure have been plotted in relation to the vertical center line through the origin of the buffer block as shown in Figure 5-4.

Figure 5-5 to 5-7 show the evaluated stress from all pressure films.

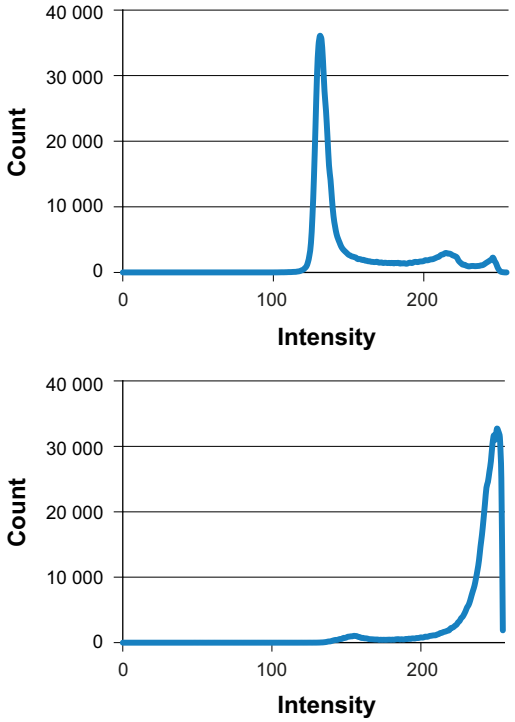

Figure 5-3. *Histogram of scan shown in Figure 5-2. The number of pixels are on the Y axis and the intensity is on the X-axis with 0 = black and 256 =white. 0 corresponds to max pressure 2.5 MPa or10 MPa depending on which film was used.*

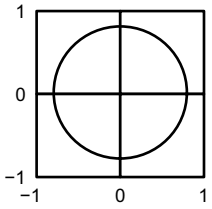

Figure 5-4. *Horizontal coordinate system used in the result plots, centered on the buffer block.*

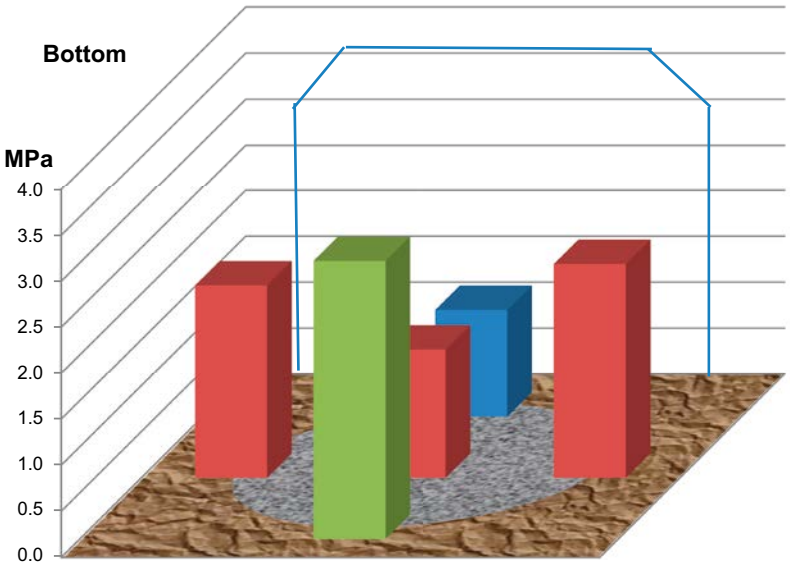

Figure 5-5. *Evaluated pressure on the buffer block.*

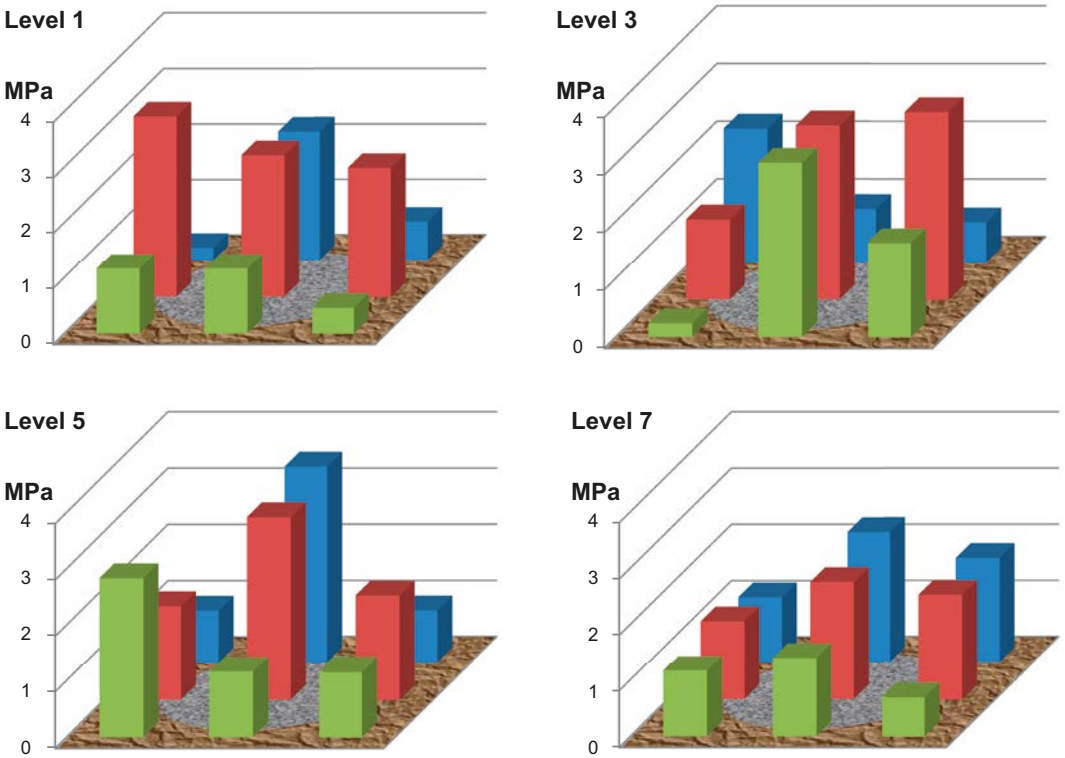

Figure 5-6. *Evaluated pressure on the different instrumented horizontal levels seen from the tunnel entrance. Level 1 is located on the first backfill block layer etc. (see Figure 3-10).*

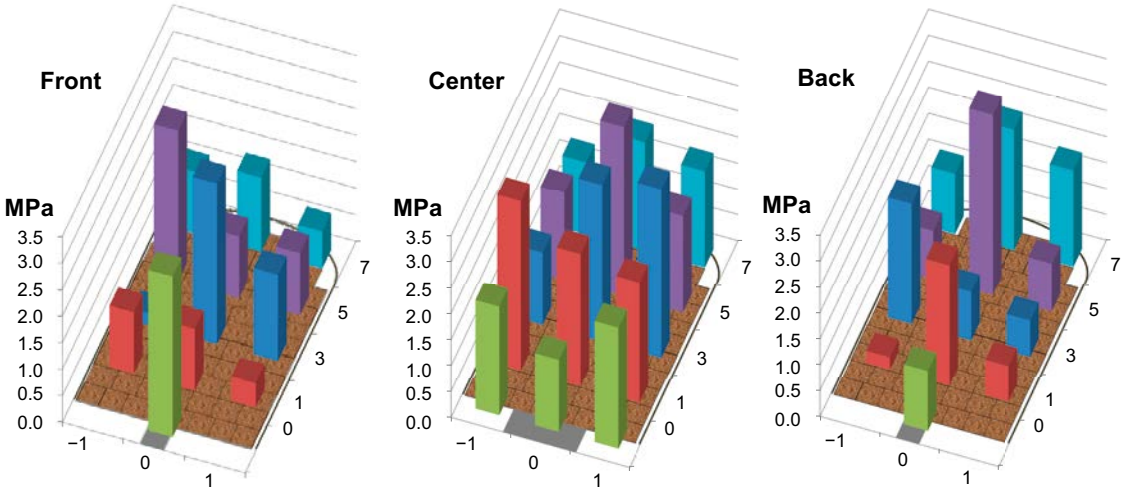

Figure 5-7. *Evaluated pressure on the different instrumented vertical levels seen from the tunnel entrance (see Figure 3-10).*

The results provided by the pressure films are very scattered, varying from less than 0.5 MPa up to more than 3.0 MPa. There is no obvious trend, i.e. no decrease with distance from the floor or distance from the center line. This is probably a sign of that the results are not very reliable. However, it could also be caused by the failure of many blocks above the simulated deposition hole, since such a failure would reduce the lateral spreading of the pressure and tend to keep the pressure rather constant inside the cracked blocks. However, this trend is contradicted by the fact that the measured pressure in the ceiling was much lower.

Lateral sliding of backfill blocks along the horizontal contact will probably cause higher readings on the films. It is, however, believed that such movements would result in tracks on the films and there were no signs of that when studying the film surfaces.

It is assessed that this type of pressure sensors could be valuable for the right type of tests. The main advantage is that no power or signal cables are needed which will facilitate installation. The disadvantages are that only a maximum pressure is registered and also that the accuracy is questionable.

6 Backfill block strength

6.1 General

The results of the excavation of the Buffer Swelling Test showed that many of the blocks located close to the simulated deposition hole had cracked as a result of the jacking force applied by the buffer block. The stress measurements also clearly showed when backfill block cracking occurred with a maximum vertical stress immediately followed by a lower residual stress that was maintained during continued upwards displacement of the buffer block. The backfill block strength is thus an important parameter that has been investigated with two different types of tests (beam tests and uniaxial compression tests) completed on the blocks installed in this test.

Technique for manufacturing bentonite backfill blocks was developed in the project "System design of backfill" (Sandén et al. 2015). Investigations have also been made to study the influence of different parameters on the block quality (Sandén et al. 2016). The data from these investigations have been used for comparison with the new results achieved in the present project.

The strength of compacted blocks is an important issue both for the handling of the blocks in order to avoid damage and pieces falling off, but also for minimizing upwards displacement caused by buffer swelling upwards into a dry tunnel with high loads acting on the backfill blocks in the tunnel.

The material used for the blocks in the BST was the bentonite Asha 2012 from India. These blocks were tested and the results described in this chapter.

6.2 Sampling

Twelve backfill blocks were chosen from the block storage at Äspö HRL for sampling. The blocks have the height 400 mm, the length 570 mm and the width 500 mm. A core with the diameter 100 mm was drilled out in the center of each of these blocks. Figures 6-1 and 6-2 show the arrangement for the sampling and a core drilled from a block.

The cores were transported to Clay Technology AB, Lund and used for testing. Two test types were performed, namely beam tests and uniaxial compression tests.The water content and dry density were determined on all samples. The water content is defined as mass of water per mass of dry substance in %. The dry mass is obtained from drying the wet specimen at 105 °C for 24h. The bulk density was calculated from the total mass of the specimen and the volume determined by weighing the specimen above and submerged into paraffin oil. The dry density was then calculated from the bulk density and water content.

For the calculation of degree of saturation the particle density ρ_s = 2 928 kg/m^3 was used for Asha 2012 (Sandén et al. 2014). The water density ρ_w = 1 000 kg/m^3 was used.

Figure 6-1. *Arrangement for the block sampling. The core drill is seen in the back of the picture and the vacuum cleaner, used for removing dust, in the front.*

Figure 6-2. *A core with diameter 100 mm has been drilled out from the block centre.*

6.3 Beam tests

6.3.1 Method

The cores taken from the backfill blocks were sliced horizontally. From these slices, rectangular beams with two different geometries were prepared by sawing. Testing involved placing the individual beam on supports and then loaded to failure by applying a constant deformation rate of 0.10 mm/min at a localized point in the middle of the beam (Figure 6-3). The load and the displacement were measured continuously.

The tensile stress (σ_t) and the strain (ε_t) were evaluated with the following equations (see Figure 6-1).

$$\sigma_t = \frac{6Qc}{4ba^2} \tag{6-1}$$

$$\varepsilon_t = \frac{a\omega 6}{c^2} \tag{6-2}$$

where

Q = vertical force

a = sample height

b = sample width

c = the length between the support points

ω = the vertical displacement at the middle of the beam

6.3.2 Test matrix

Three test series have been performed with specimens from the Asha 2012 blocks:

1. Test series 1: Beams with the dimensions $10 \times 20 \times 40$ mm. Two beams were prepared from each of the blocks 2, 3, 8 and 9. In total 8 beams were tested.
2. Test series 2: Beams with the dimensions $20 \times 20 \times 80$ mm. Two beams were prepared from each of the blocks 1–12. In total 23 beams were tested (one beam from block no. 8 was damaged and could not be used).
3. Test series 3: Beams with the dimensions $20 \times 20 \times 80$ mm. Repetition of test series 2. In total 22 beams were tested (the two beams from block no. 8 were damaged and could not be used).

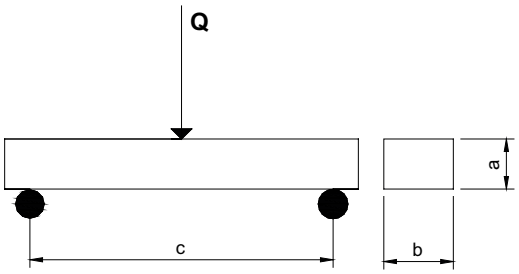

Figure 6-3. *Test arrangement for determination of the tensile strength.*

6.3.3 Results

General

The beams used in the test were sawed out by use of a band saw. Most of the beams were prepared without any problems. However, the samples made from block no. 8 were rather brittle and it was not possible to achieve beams of good quality.

Figure 6-4 shows a typical behaviour of the beams tested. A small fracture develops close to the mid-point and finally the beam is divided in two pieces, Figure 6-5. After the tests the pieces of beam were used to determine the density and water content. Figure 6-4 and Figure 6-5 also show how the original granularity of the crushed raw bentonite used in manufacturing the backfill blocks remain visible (individual granules still visible in the beam) and that the fracture is developed between the granules.

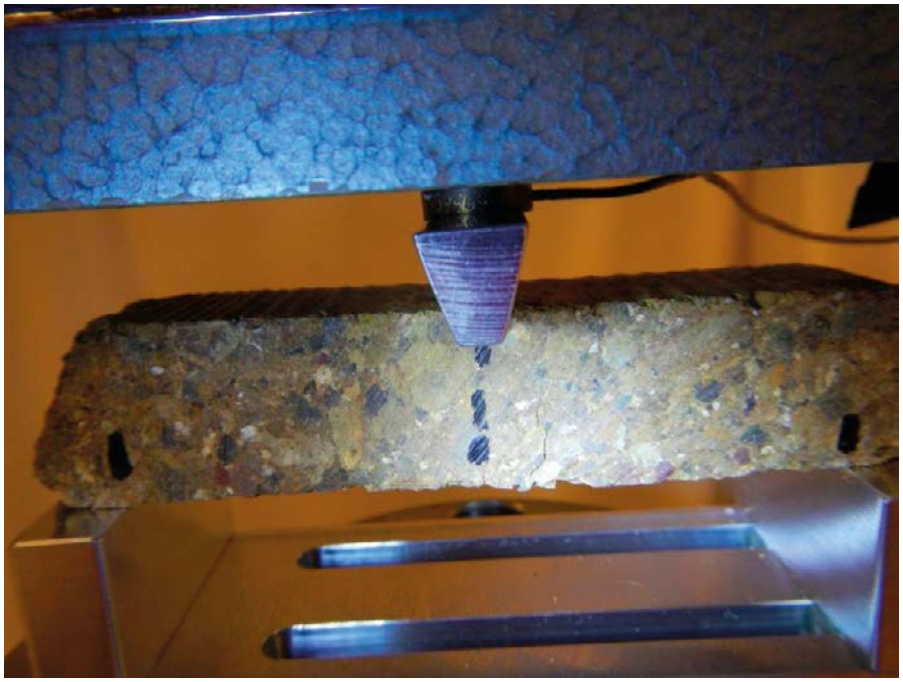

Figure 6-4. *The photo shows a fracture developing close to the midpoint of the beam during a test.*

Figure 6-5. *Photo showing a beam after the test.*

Determined block strength

The results from the tests performed in three test series are presented in Table 6-1 to 6-3.

Table 6-1. Compilation of results from the tests performed in test series 1.

Test ID	Water content %	Dry density kg/m^3	Void ratio	Max. tensile stress kPa	Strain at failure %
Block 2A	19.4	1 661	0.746	181	0.613
Block 2B	19.4	1 659	0.748	264	0.657
Block 3A	19.9	1 669	0.737	238	0.885
Block 3B	20.2	1 659	0.748	329	0.571
Block 8A	19.3	1 657	0.750	190	1 049
Block 8B	19.3	1 678	0.728	177	0.643
Block 9A	18.7	1 680	0.727	269	0.405
Block 9B	20.2	1 667	0.740	222	0.542

Table 6-2. Compilation of results from the tests performed in test series 2.

Test ID	Water content %	Dry density kg/m^3	Void ratio	Max. tensile stress kPa	Strain at failure %
Block 1A	20.1	1 663	0.744	288	0.401
Block 1B	20.0	1 672	0.734	402	0.304
Block 2A	19.4	1 660	0.747	162	0.368
Block 2B	19.3	1 654	0.753	138	0.308
Block 3A	19.8	1 664	0.743	374	0.529
Block 3B	20.0	1 662	0.745	357	0.508
Block 4A	19.9	1 669	0.737	76	0.306
Block 4B	19.8	1 667	0.739	200	0.244
Block 5A	20.0	1 662	0.745	292	0.568
Block 5B	19.7	1 670	0.737	353	0.431
Block 6A	19.5	1 678	0.729	117	0.278
Block 6B	19.6	1 687	0.719	179	0.294
Block 7A	19.4	1 666	0.740	321	0.336
Block 7B	19.4	1 656	0.751	301	0.398
Block 8A	19.4	1 653	0.754	164	0.251
Block 8B					
Block 9A	20.0	1 661	0.746	310	0.356
Block 9B	20.4	1 654	0.754	223	0.310
Block 10A	19.6	1 692	0.714	243	0.269
Block 10B	20.0	1 683	0.723	298	0.395
Block 11A	19.7	1 677	0.730	305	0.273
Block 11B	19.8	1 673	0.733	124	0.323
Block 12A	19.8	1 659	0.748	289	0.278
Block 12B	20.0	1 664	0.743	427	0.410

Table 6-3. Compilation of results from the tests performed in test series 3.

Test ID	Water content %	Dry density kg/m^3	Void ratio	Max. tensile stress kPa	Strain at failure %
Block 1A	19.5	1679	0.727	343	0.279
Block 1B	19.4	1685	0.721	369	0.423
Block 2A	18.7	1675	0.731	294	0.447
Block 2B	18.4	1678	0.728	261	0.478
Block 3A	19.4	1676	0.730	331	0.276
Block 3B	19.3	1676	0.730	326	0.287
Block 4A	19.2	1668	0.739	405	0.407
Block 4B	19.1	1675	0.731	428	0.475
Block 5A	19.5	1673	0.734	490	0.460
Block 5B	19.5	1667	0.740	397	0.340
Block 6A	19.9	1666	0.741	205	0.383
Block 6B	19.0	1673	0.733	328	0.388
Block 7A	19.4	1669	0.738	307	0.382
Block 7B	18.8	1673	0.733	288	0.428
Block 8A					
Block 8B					
Block 9A	19.6	1667	0.739	362	0.356
Block 9B	19.3	1673	0.733	302	0.412
Block 10A	19.8	1678	0.728	441	0.461
Block 10B	19.6	1684	0.722	406	0.297
Block 11A	19.6	1673	0.733	363	0.527
Block 11B	19.9	1671	0.735	289	0.341
Block 12A	19.6	1672	0.735	323	0.400
Block 12B	19.3	1663	0.743	272	0.327

Figure 6-6 shows the results from the tests with the tensile strength (red dots) plotted versus the dry density. The results are presented together with results from earlier laboratory tests performed on the same material (Asha 2012) (Sandén et al. 2014). As shown in the graph, the achieved block densities are low and this has influenced the strength of the blocks which also is low compared to the earlier results. The results from this investigation have also been plotted in Figure 6-7 together with results from another investigation where both Asha and Ibeco bentonites were tested (Sandén et al. 2016). In this graph, the results are plotted versus the void ratio. As shown in the graph, all results from this investigation are gathered below a tensile strength of 500 kPa and they are in agreement with the earlier results for this water content and at this void ratio if the trend lines are extrapolated.

The results from all three test series are also presented in a graph (Figure 6-8), where the maximum tensile strength is plotted versus the individual block number. The variation in results is very high ranging from 76 kPa to 490 kPa.

6.4 Uniaxial compression tests

6.4.1 General

The unconfined compressive strength was determined using unconfined undrained uniaxial compression tests, which in this test is equal to the maximum deviator stress at failure. During an unconfined compression test a cylindrical specimen is placed in a load frame where the vertical load on its ends is increased via constant rate of strain until mechanical failure occurs.

The same large backfill blocks 1–12 used for supplying materials for the beam tests were also used for the uniaxial compression tests. The material in the blocks was the bentonite Asha 2012 from India. An investigation has earlier been made to determine the effect of the specimen shape.

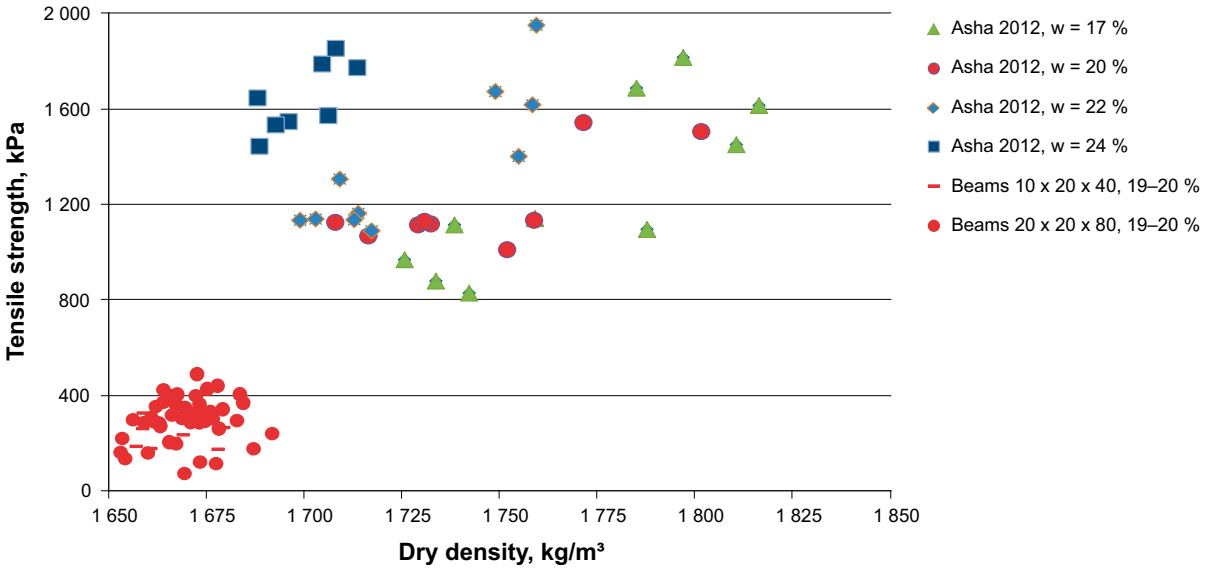

Figure 6-6. *The maximum tensile strength plotted versus dry density for samples taken from the actual blocks tested ("Beams 10 × 20 × 40 mm" and "Beams × 20 × 80 mm") and from earlier investigations (Sandén et al. 2014).*

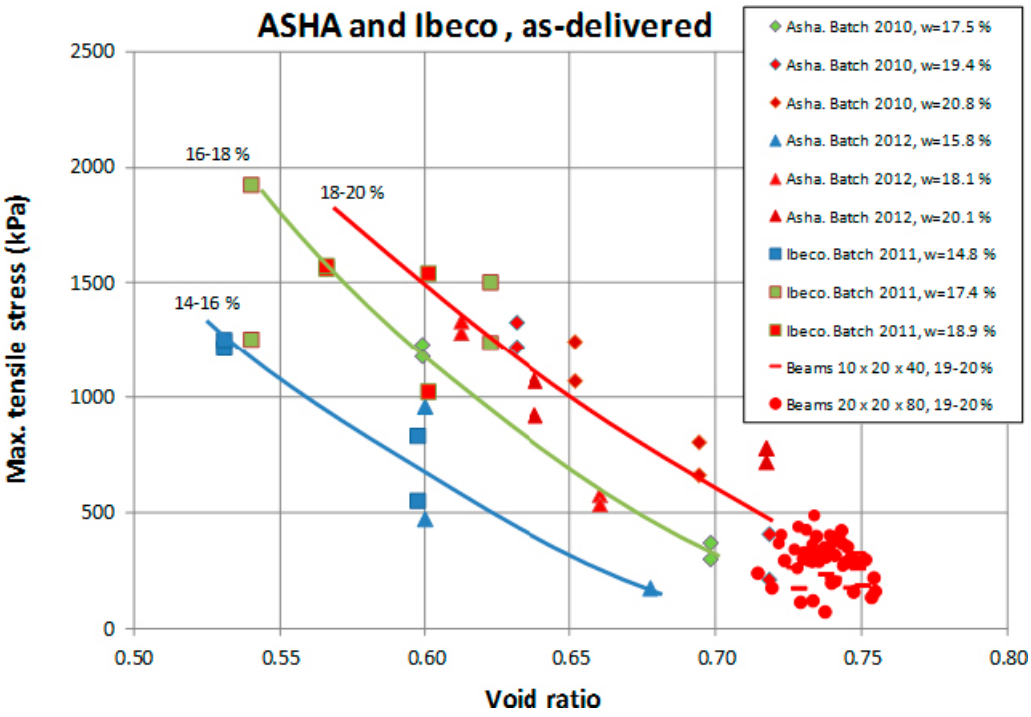

Figure 6-7. *The maximum tensile strength plotted versus void ratio for samples taken from the actual blocks tested ("Beams 10 × 20 × 40" and "Beams × 20 × 80") and from earlier investigations (Sandén et al. 2016).*

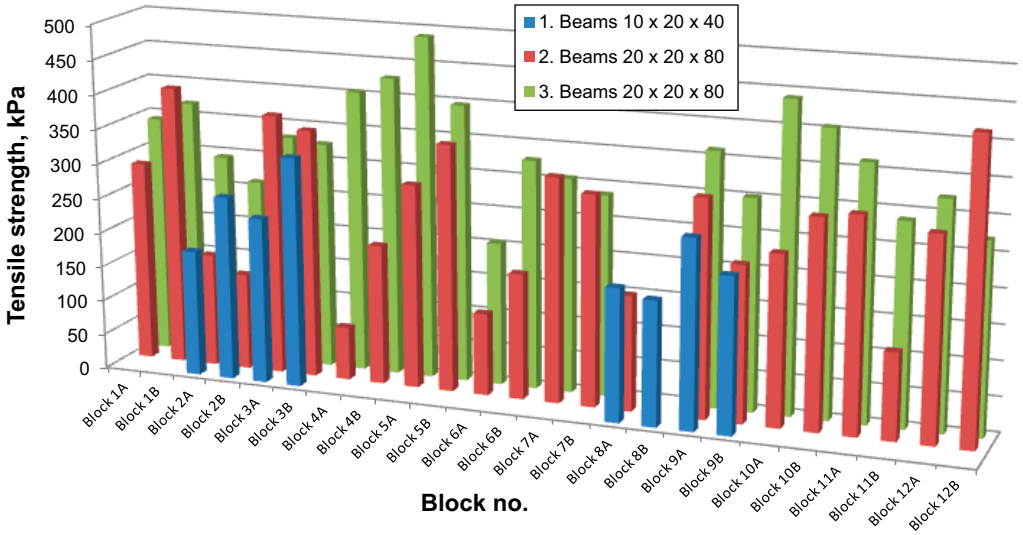

Figure 6-8. *The graph shows the tensile strength of all samples tested, plotted versus block number.*

6.4.2 Techniques

Unconfined compression test

The unconfined compression test is an experimentally simple method where a cylindrical specimen is compressed axially under a constant rate of strain with no radial confinement or external radial stress. The method has been used in several studies (e.g. Börgesson et al. 2003, Dueck 2010, Dueck et al. 2011, Svensson et al. 2011). The specimens tested are placed in a mechanical press where a constant rate of deformation is applied to the specimen. During the test the deformation and the applied force are measured by means of a load cell and a deformation transducer.

Preparation of specimen

The method is usually used for saturated cylindrical specimens with a height which is double the diameter. In the test series presented in this report, unsaturated specimens with a rectangular cross section were used. Rectangular shaped specimens were used since these were possible to prepare by sawing, which were considered the best available method for sampling of the unsaturated Asha 2012 blocks containing large granules. The specimens were sampled from the larger cylinders of Asha 2012 and sawn to the chosen dimensions wh-ere the height was double the size of the side of the square cross section. Photos of these specimens are presented in Appendix 5.

Some additional specimens were also prepared of compacted MX-80 for comparison.

Test procedure

The specimens were placed in a mechanical press and the compression was run at a constant deformation rate of 0.32 mm/min (which corresponds to 0.8 %/min for a specimen with the height 40 mm), a test procedure which has been used also in earlier test series (see e.g. Dueck et al. 2011). After failure the water content and density were measured.

Evaluation of test results

The deviator stress q (kPa) was calculated as the ratio of the measured vertical load and the initial cross section area. No correction is made for the change in the cross section area in the calculated q since the specimen failed after very small deformation (about 2 % strain). The strain ε (%) was calculated as the ratio between the change in length and the initial height of the specimen.

6.4.3 Test results

A total of 36 samples were trimmed and tested using the unconfined compression test described above in Section 6.4.2. From the larger block samples of Asha 2012 (see Section 6.2) specimens for the actual tests were sawn and tested in four series (1, 2, 3 and 4). Samples from each block were tested. Blocks 1–6 were included in series 4 and blocks 7–12 were used in series 1. However, block 8 was not possible to sample with the chosen method and dimension and no samples were taken from this block (the block was too brittle to recover intact specimens from, as for the beam tests). In addition to series 1 and 4, two additional series with samples from blocks 7–12 were run to study the scatter (series 2) and the influence of size (series 3) on the results obtained.

The plotted results mark whether the sample is taken from blocks 1–6 (diamond) or blocks 7–12 (circles). For each marker the colours (red, yellow, green, blue, brown and grey) are used to distinguish between the different blocks.

Since the samples were sawn from larger blocks, the cross section varied slightly over the sample height. This is why the cross section (and the corresponding side) of each specimen was c-alculated as an average from the bulk density determined after the test and the weight and height determined before the test.

In addition to the test results more details can be found in Appendices 3–5. The results of tests to determine the effects of specimen shape (cylindrical versus rectangular) of MX-80 are provided in Appendix 5. If the same lack of shape-effect exists for the rectangular Asha 2012 specimens then the test results described in this report can be used in numerically evaluating buffer-backfill interactions.

In Figure 6-9 the resulting maximum deviator stress q_{max} is shown as a function of the dry density. Two samples were taken from each block except from block 8 where no sample was taken and block 9 where only one sample was taken. The dry density of the samples had values between 1 650 and 1 700 kg/m^3 and the maximum deviator stress recorded varied between 1 250 and 2 500 kPa.

In Figure 6-10 the results from more tests on samples from blocks 6 through 12 are shown. These additional tests were run in order to study the scatter and the influence of the size of the specimen. The largest scatter in q_{max} was seen in samples from blocks 9 and 10 and the largest scatter in density was seen in blocks 7 and 12. No systematic deviation occurred in the results from samples of the larger size, with the side 35 mm and the height 70 mm, compared to the more common dimension used in the other series, with the side 20 mm and the height 40 mm. All results on Asha 2012 are shown in Table 6-4, where the side of the square section of the specimens were back-calculated from the bulk density together with the weight and height of the actual specimen. The deviator stress plotted as a function of strain resulting from all tests are shown in Appendix 3. Photos of some of the tested samples are shown in Appendix 4.

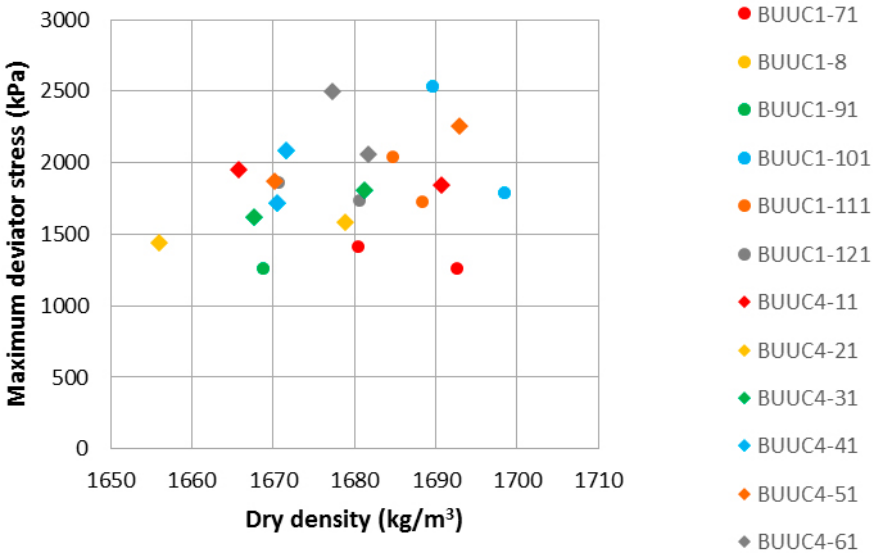

Figure 6-9. *Results of series 1 (circles) and 4 (diamonds). Maximum deviator stress determined on specimens sampled from each of the blocks 1–12 except block 8 which was brittle to handle. The side of the square cross section and the height of the specimens were 20 and 40 mm, respectively.*

Table 6-4. Results from unconfined compression tests. The dry density and water content determined after the tests and the evaluated maximum deviator stress q_{max} are shown as well as the dimensions of the specimens.

Test ID	Block	Dimensions		Final values			At shearing	Remarks
		height mm	side mm	dry density kg/m^3	w %	Sr %	max q kPa	
BUUC1-71	7	38.4	20.0	1690	19.3	78	1260	
BUUC1-72	7	37.4	20.1	1680	19.3	76	1410	
BUUC1-8	8							No sample
BUUC1-91	9	39.9	19.7	1670	18.8	73	1270	
BUUC1-101	10	39.6	20.2	1700	19.6	79	1790	
BUUC1-102	10	39.6	20.5	1690	19.6	78	2540	
BUUC1-111	11	39.8	19.9	1690	19.5	78	1730	
BUUC1-112	11	39.6	20.0	1680	20	79	2040	
BUUC1-121	12	39.6	20.2	1670	19.7	77	1870	
BUUC1-122	12	39.1	19.5	1680	19.5	77	1740	
BUUC2-71	7	39.1	20.0	1680	19.3	76	1690	
BUUC2-72	7	39.1	19.6	1700	18.6	76	1640	
BUUC2-8	8							No sample
BUUC2-91	9	39.5	19.0	1690	19.5	78	1190	
BUUC2-92	9	39.9	18.8	1690	20.1	80	1880	
BUUC2-101	10	40.2	20.1	1690	19.5	78	2450	
BUUC2-102	10	40.1	19.8	1700	19.6	80	2020	
BUUC2-111	11	40.5	19.3	1680	19.7	78	1590	
BUUC2-112	11	40.3	19.2	1700	20	81	1670	
BUUC2-121	12	41.3	20.1	1680	19.6	77	1500	
BUUC2-122	12	39.4	19.0	1690	19.7	79	1580	
BUUC3-71	7	70.8	35.1	1670	19.3	76	1730	
BUUC3-81	8							No sample
BUUC3-91	9	70.8	34.2	1680	20.2	80	1630	
BUUC3-101	10	69.7	33.6	1710	19.6	80	2100	
BUUC3-111	11	70.9	34.3	1680	19.8	78	1410	
BUUC3-121	12	69.6	34.2	1660	19.7	75	1580	
BUUC4-11	1	39.3	19.0	1690	19.6	78	1840	
BUUC4-12	1	38.8	19.5	1670	19.9	77	1950	
BUUC4-21	2	40.3	19.0	1660	19.7	75	1450	
BUUC4-22	2	40.7	19.1	1680	19.3	76	1580	
BUUC4-31	3	40.6	20.0	1680	20.2	80	1810	
BUUC4-32	3	40.5	19.7	1670	19.6	76	1620	
BUUC4-41	4	39.9	19.8	1670	19.5	76	1720	
BUUC4-42	4	40.1	19.7	1670	19.7	77	2090	
BUUC4-51	5	39.3	19.1	1670	20.1	78	1870	
BUUC4-52	5	39.2	19.3	1690	19.4	78	2250	
BUUC4-61	6	38.6	19.4	1680	19.6	77	2500	
BUUC4-62	6	39.5	19.7	1680	19.5	77	2060	

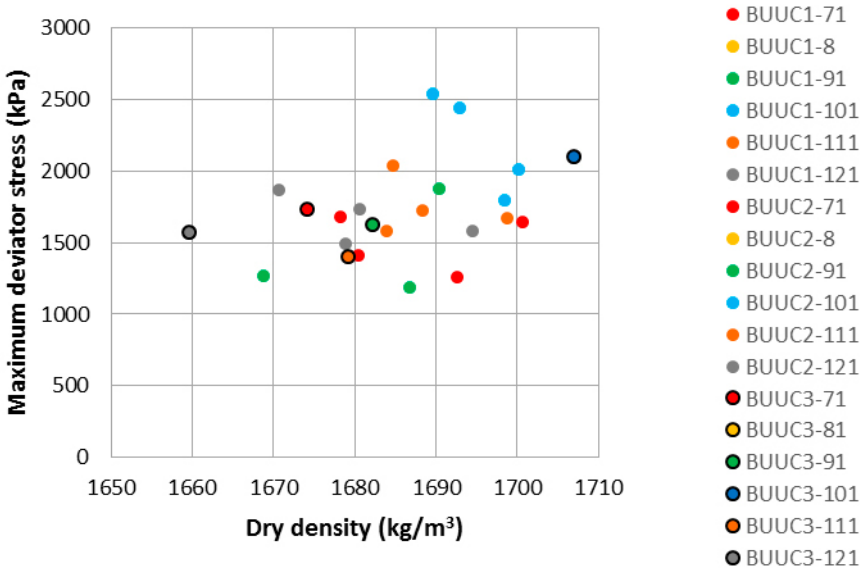

Figure 6-10. *Maximum deviator stress determined in series 1, 2 and 3 on samples from blocks 7–12, except block 8. The colours (red, yellow, green, blue, brown, grey) show the blocks (7, 8, 9, 10, 11, 12). No marker line is used for specimens with the side 20 mm while black marker lines are used for specimens with the side 35 mm.*

6.4.4 Comments

The maximum deviator stress of samples from each of the blocks 1–12, shown in Figure, had an average of 1 828 kPa with the standard deviation 339 kPa. The average dry density was 1 679 kg/m^3 with the standard deviation 11 kg/m^3.

The determination of density was made by weighing the samples above and submerged into paraffin oil. This method for density measurements works well for small irregularly-shaped specimens but when the degree of saturation is low the density may be slightly overestimated.

In Figure 6-11 the results from Figure 6-9 are plotted together with results from a previous study made on the same material (Sandén et al. 2014). In that study compacted cylindrical specimens with a diameter of 35 mm were tested with the unconfined compression test method and the deformation rate 0.09 mm/min.

The differences between the two studies were the size of the specimens, the form of the cross section, the deformation rate and the preparation of the specimens. In the present study two different specimen sizes were tested and no large difference between the results for the prismatic specimens could be seen (Figure 6-9 and Figure 6-10). The influence of the shape of the cross section area was studied on specimens of MX-80 (cylindrical and rectangular specimens). The results are presented in Appendix 5 and showed no obvious difference in results for circular and square cross sections. One test series was run at the slightly lower rate of strain 0.09 mm/min but the difference in the strength obtained for 0.09 versus 0.32 mm/min was too small to attribute any influence of the rate of strain.

The specimens used in the current study were sampled from large blocks originally prepared at a water content of 20 %. If the results from the current test series are compared to the results from the previously mentioned study by Sanden et al. (2014), despite the differences commented on above, the results from the current study seems to follow the same trend as the specimens in the previous study prepared at the same water content, i.e.20 %. The trend is illustrated with a dotted line in Figure 6-11. This might indicate an influence of degree of saturation, which has not been seen earlier in results from specimens of MX-80 (Dueck 2010).

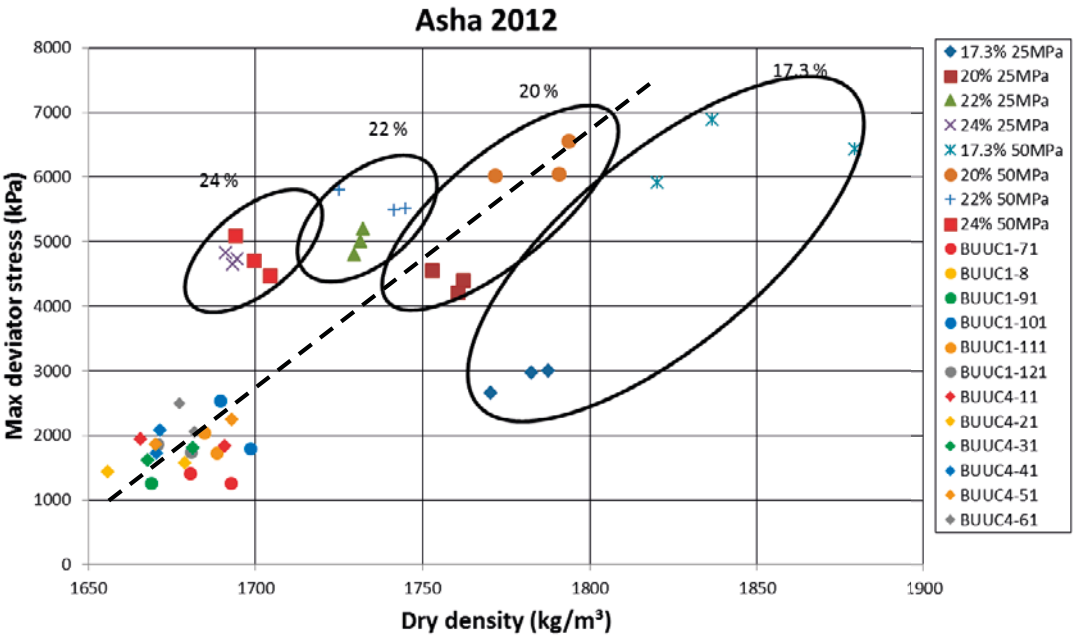

Figure 6-11. *Test results from the present study plotted into a diagram from Sandén et al. (2014). (Figure 6-10 in report R-13-8).*

7 Final remarks and preliminary conclusions

The final detailed evaluation of the observations made in the BST will be done in another report dealing with the modelling of the test. Some preliminary conclusions and comments have been compiled and are provided for in this chapter.

7.1 Simulated buffer swelling

The buffer swelling below the top-most block of buffer (block in contact with backfill) was simulated by pressing a buffer block upwards in steps of 5 or 10 mm every 15 minutes. This buffer block therefor had the mechanical properties of the as-built buffer and that was being pushed upwards by underlying, hydrating buffer as an intact mass that did not discernibly interact with the walls of the deposition hole. This uppermost block also saw not water uptake itself.

The displacement measured by four transducers located on the jacking plate below the buffer block was uniform while the load varied somewhat between the four hydraulic jacks. The variation in load is judged to be caused by several reasons e.g. the fact that four jacks were used (one more than required), uneven location of the backfill blocks and the failure of some backfill blocks.

The total buffer block displacement upwards was approx. 150 mm and the maximum pressure approx. 1 800 kPa was reached after 75–80 mm displacement after which a residual stress of 1 200–1 400 was measured.

7.2 Pressure on rock walls and between the backfill blocks

7.2.1 Pressure on rock walls

Only two of the five sensors positioned on the rock above the deposition hole (at different positions) registered a significant pressure increase. At the midpoint above the deposition hole, on the rock ceiling, a maximum pressure of approx. 350 kPa was registered. At the left corner, in the transition between the ceiling and the wall a pressure of approx. 300 kPa was registered. The pressure on these two sensors increased stepwise according to changes in the applied buffer displacement.

7.2.2 Pressure between backfill blocks

The pressure between the backfill blocks was measured by special indicators (plastic film), registering the maximum pressure they have been exposed to. These indicators were placed at 41 different positions. The results from these measurements were rather inconsistent. They showed a strong variation and a lack in the expected stress reduction with distance from the floor. It is therefore not clear whether the trends and magnitudes indicated by this material are real.

7.3 Test termination

The backfill blocks above and around the simulated deposition hole were carefully examined during the excavation. The following observations were made:

- The backfill blocks just above the deposition hole had widely sheared at the buffer block periphery.
- The blocks in the three first layers had large damage while the blocks in the next four layers had cracked in some directions.
- The blocks in the four uppermost layers had very small damage and seemed to mainly have been displaced within the tunnel (tilted or shifted).

- The backfill block layers had a very evident “bow shape” above the deposition hole due to the larger vertical displacement in the centre of the block-filled volume than in the periphery. The outermost blocks, at the walls, seemed to have been moved outwards against the rock wall. This behaviour was more evident on the right side of the tunnel.
- The block stack was almost unaffected of the buffer heaving in the inner and outer parts of the tunnel at some distance from the simulated deposition hole.
- It seemed as if the applied load from the simulated buffer heaving had not been laterally distributed in the block stack. Instead the backfill blocks had been sheared off at many positions above and immediately adjacent to the buffer. This is in agreement with the pressure film measurements but not in agreement with the low pressure measured in the roof. If the often used assumption in soil mechanics of a lateral spreading of 1:2 is applied the loss in vertical stress would be a factor of about 15, which would yield an average stress at the roof of 110–120 kPa. The measured stress in the centre of the ceiling was about 300 kPa, which is higher but still in the right range considering that the actual stress is not constant but will decrease with distance from the centre.

7.4 Backfill compression

The applied total buffer vertical displacement of approx. 150 mm has according to the test observations been distributed in the different parts of the backfill above the simulated deposition hole as follows:

- The 70–90 mm thick pellet layer in the floor between the buffer block and the bottom backfill block has been compressed about 30 mm.
- The 430 mm thick pellet layer in the roof between the upper backfill block and the rock ceiling has been compressed about 40 mm
- The backfill block section (compression of slots, elastic compression and movements in horizontal direction) has been compressed about 80 mm.

7.5 Shear strength and cracking of backfill block

Measurements of the uniaxial compression strength and the tensile strength of the backfill blocks show that the strength is rather low compared with previously obtained backfill block measurements. This is mainly due to the low density and relatively low water content of the BST blocks as compared to previously measured materials. The scatter in the measurement values can also be attributed to the large granules in the bentonite, whose presence will adversely affect strength and deformation behaviour However, the average uniaxial compression strength in the lab tests was about 1 600 kPa, which agrees very well with the applied peak axial stress at the BST reached just before failure of many of the backfill blocks. A preliminary conclusion is that the resistance to upwards swelling can be substantially improved if the backfill blocks were made to higher density and thereby would exhibit a higher compression strength.

7.6 Preliminary evaluation of the test

The test has been modelled and the results of these modelling are reported in two reports: Börgesson and Hernelind (2016) and Martino et al. (2016). These reports also include evaluation of the test, comparison between modelled and measured results and evaluation of the modelling technique, the material models and the parameters. In this way the purpose of the test has been very well fulfilled and the results up to 80 mm displacement of the buffer block agreed well with measurements. The only problem and disappointment was that the blocks cracked, which had not been expected. This led to that the data after 80 mm displacement was difficult to use and also shadowed the final results at excavation. However, the Buffer Swelling Test revealed a weakness that had not been considered and showed that the backfill bock quality is of outmost importance.

References

SKB's (Svensk Kärnbränslehantering AB) publications can be found at www.skb.com/publications.

Andersson L, Sandén T, 2012. Optimization of backfill pellet properties. ÅSKAR DP2. Laboratory tests. SKB R-12-18, Svensk Kärnbränslehantering AB.

Arvidsson A, Josefsson P, Eriksson P, Sandén T, Ojala M, 2015. System design of backfill. Project results. SKB TR-14-20, Svensk Kärnbränslehantering AB.

Börgesson L, Hernelind J, 2016. Modelling of the mechanical interaction between the buffer and the backfill in KBS-3V. Modelling results 2015. SKB TR-16-08, Svensk Kärnbränslehantering AB.

Börgesson L, Johannesson L-E, Hernelind J, 2003. Earthquake induced rock shear through a deposition hole. Effect on the canister and the buffer. SKB TR-04-02, Svensk Kärnbränslehantering AB.

Dueck A, 2010. Thermo-mechanical cementation effects in bentonite investigated by unconfined compression tests. SKB TR-10-41, Svensk Kärnbränslehantering AB.

Dueck A, Johannesson L-E, Kristensson O, Olsson S, 2011. Report on hydro-mechanical and chemical-mineralogical analyses of the bentonite buffer in Canister Retrieval Test. SKB TR-11-07, Svensk Kärnbränslehantering AB.

Martino L, Börgesson L, Keto P, 2016. Numerical modelling of the Buffer Swelling Test in Äspö HRL. Validation of numerical models with the ÅSKAR test data. SKB TR-17-03, Svensk Kärnbränslehantering AB.

Sandén T, Olsson S, Andersson L, Dueck A, Jensen V, Hansen E, Johnsson A, 2014. Investigation of backfill candidate materials. SKB R-13-08, Svensk Kärnbränslehantering AB.

Sandén T, Andersson L, Jensen V, 2015. System design of backfill. Full scale production test of backfill blocks. SKB P-14-24, Svensk Kärnbränslehantering AB.

Sandén T, Nilsson U, Andersson L, 2016. Investigation of parameters influencing bentonite block quality. Laboratory investigation. SKB P-16-06, Svensk Kärnbränslehantering AB.

Svensson D, Dueck A, Nilsson U, Olsson S, Sandén T, Lydmark S, Jägerwall S, Pedersen K, Hansen S, 2011. Alternative Buffer Material. Status of the ongoing laboratory investigation of reference materials and test package 1. SKB TR-11-06, Svensk Kärnbränslehantering.

Measurement of block positions

PROJEKT - KBP1003
Tunnel TASS
Kontroll inmätning av bentonintblok
inmätning utfört av: S.Karamehmedovic - GEOCON

Pkt	Datum: 2014-02-27				Datum: 2014-03-18				avvikelse [mm]			Rad. differens	Rad. differens 3d	anmärkning
	X	Y	Z	Kod	Pkt	X	Y	Z	Kod	X	Y	Z			
1	7204.408	1900.349	-447.453	REF	1	förstörd									
2	7204.852	1899.969	-447.463	REF	2	7204.873	1899.998	-447.349	REF	21	29	114	36	120	
3	7205.444	1899.467	-447.487	REF	3	7205.510	1899.474	-447.415	REF	66	7	72	66	98	
4	7204.343	1899.977	-446.699	REF	4	7204.341	1899.988	-446.564	REF	-2	11	135	11	136	
5	7204.750	1899.630	-446.669	REF	5	7204.817	1899.664	-446.572	REF	67	34	97	75	123	lossnat
6	7205.332	1899.131	-446.687	REF	6	7205.378	1899.124	-446.619	REF	46	-7	68	47	82	
7	7203.971	1899.869	-445.912	REF	7	7203.964	1899.871	-445.861	REF	-7	2	51	7	52	
8	7204.459	1899.450	-445.897	REF	8	7204.457	1899.445	-445.849	REF	-2	-5	48	5	48	
9	7205.012	1898.976	-445.877	REF	9	7205.043	1898.970	-445.818	REF	31	-6	59	32	67	
10	7203.800	1899.682	-445.045	REF	10	7203.793	1899.677	-445.001	REF	-7	-5	44	9	45	
11	7204.390	1899.174	-445.043	REF	11	7204.401	1899.167	-444.993	REF	11	-7	50	13	52	
12	7204.945	1898.695	-445.058	REF	12	7204.954	1898.682	-445.006	REF	9	-13	52	16	54	
13	7203.440	1899.466	-444.258	REF	13	7203.429	1899.457	-444.216	REF	-11	-9	42	14	44	
14	7204.056	1898.937	-444.256	REF	14	7204.052	1898.928	-444.215	REF	-4	-9	41	10	42	
15	7204.792	1898.302	-444.283	REF	15	7204.792	1898.292	-444.242	REF	0	-10	41	10	42	
16	7203.435	1899.227	-443.446	REF	16	7203.433	1899.224	-443.410	REF	-2	-3	36	4	36	
17	7204.006	1898.737	-443.456	REF	17	7204.004	1898.730	-443.419	REF	-2	-7	37	7	38	
18	7204.537	1898.280	-443.463	REF	18	7204.537	1898.271	-443.425	REF	0	-9	38	9	39	
	Datum: 2014-03-06				Datum: 2014-03-07					avvikelse [mm]			Rad. differens	Rad. differens 3d	anmärkning
	bentonitblock framsida				bentonitblock framsida					X	Y	Z			
19	7208.546	1904.459	-446.749	REF	19	7208.546	1904.460	-446.747	REF	0	1	2	1	2	
20	7207.882	1904.977	-445.976	REF	20	7207.882	1904.978	-445.973	REF	0	1	3	1	3	
21	7208.408	1904.526	-445.985	REF	21	7208.408	1904.527	-445.983	REF	0	1	2	1	2	
22	7209.150	1903.893	-445.965	REF	22	7209.150	1903.893	-445.963	REF	0	0	2	0	2	
23	7207.585	1905.194	-445.049	REF	23	7207.584	1905.195	-445.046	REF	-1	1	3	1	3	
24	7208.421	1904.476	-445.183	REF	24	7208.421	1904.477	-445.181	REF	0	1	2	1	2	
25	7209.349	1903.691	-445.099	REF	25	7209.349	1903.692	-445.096	REF	0	1	3	1	3	
26	7207.651	1905.090	-444.360	REF	26	7207.652	1905.091	-444.357	REF	1	1	3	1	3	
27	7208.359	1904.482	-444.370	REF	27	7208.360	1904.483	-444.367	REF	1	1	3	1	3	
28	7209.398	1903.607	-444.345	REF	28	7209.398	1903.608	-444.343	REF	0	1	2	1	2	

Oil pressure in jacks and displacement data

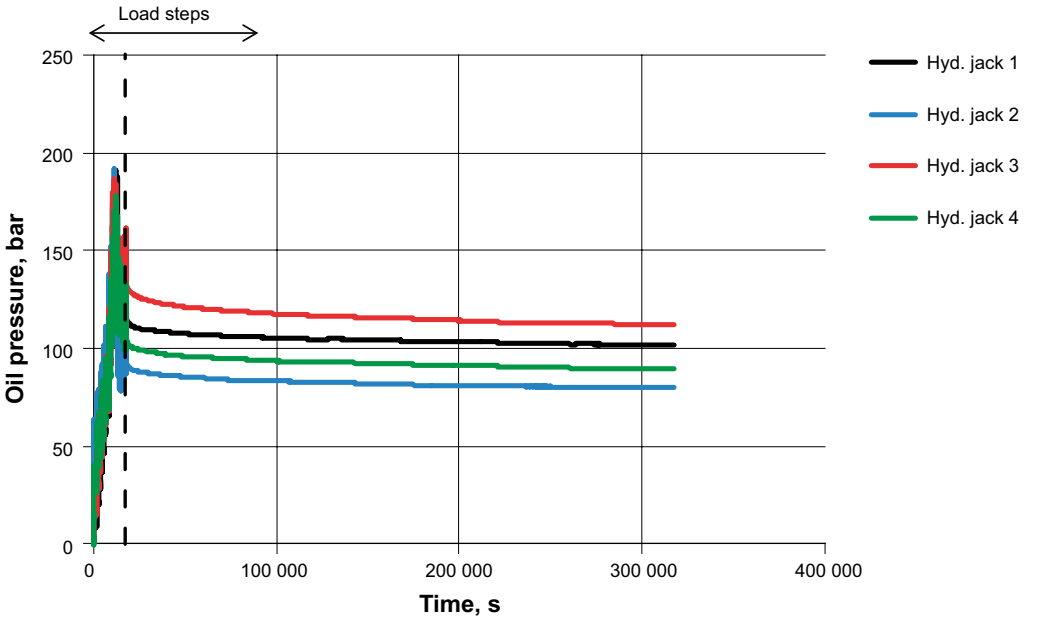

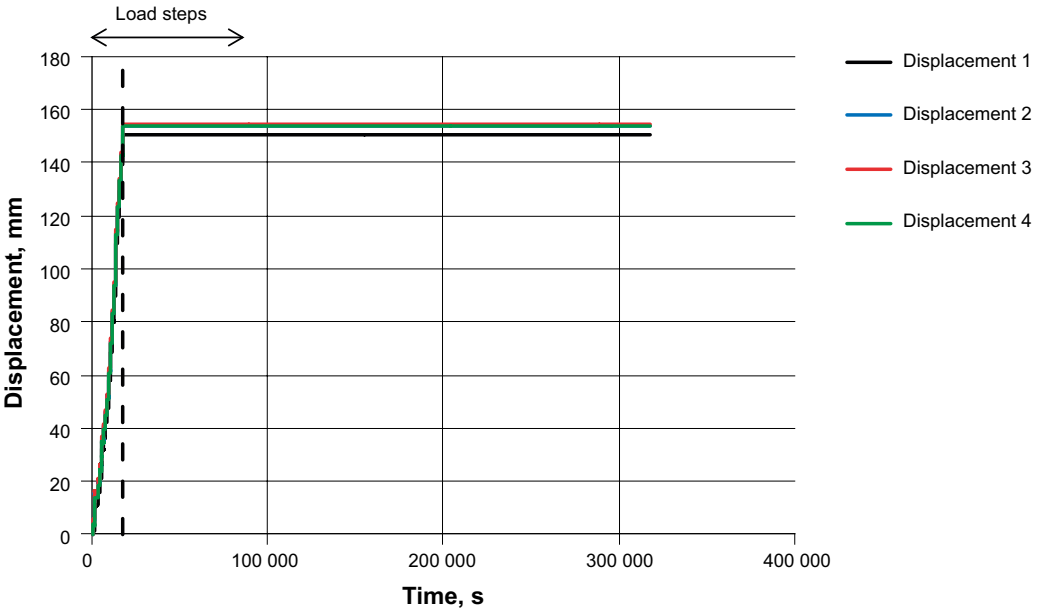

Appendix 3

Deviator stress as a function of strain

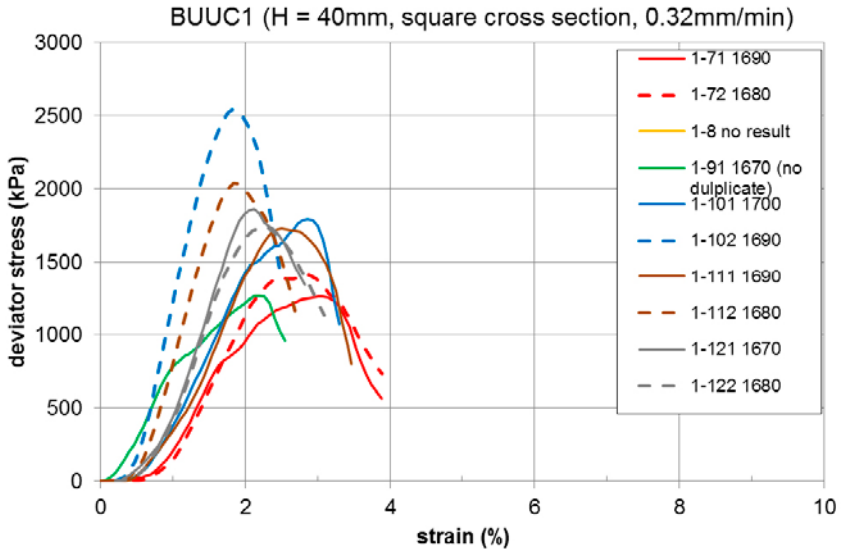

Figure A3-1. *Deviator stress as a function of strain resulting from test series 1 (BUUC1). A total of 9 samples from blocks 7–12, not from block 8, were tested. The deformation rate was 0.32 mm/min and the specimens had square cross section with a side of 20 mm and a height of 40 mm.*

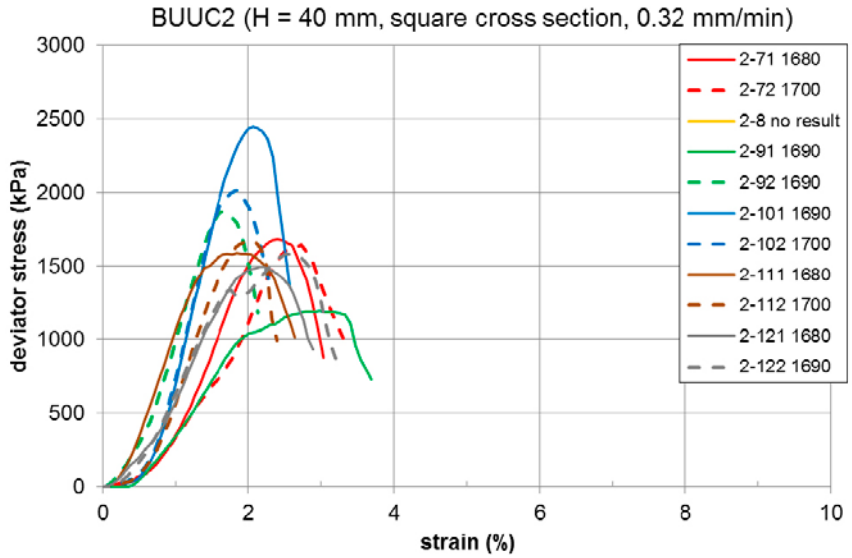

Figure A3-2. *Deviator stress as a function of strain resulting from test series 2 (BUUC2). A total of 10 samples from blocks 7–12, not from block 8, were tested. The deformation rate used was 0.32 mm/min and the specimens had square cross section with a side of 20 mm and a height of 40 mm.*

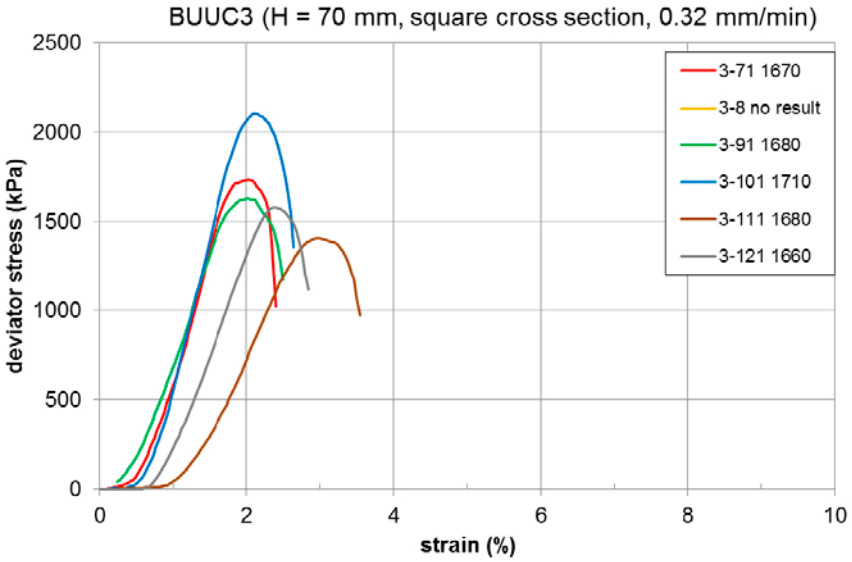

Figure A3-3. *Deviator stress as a function of strain resulting from test series 3 (BUUC3). A total of 5 samples from blocks 7–12, not from block 8, were tested. The deformation rate of the tests was 0.32 mm/min and the specimens had square cross section with a side of 35 mm and a height of 70 mm.*

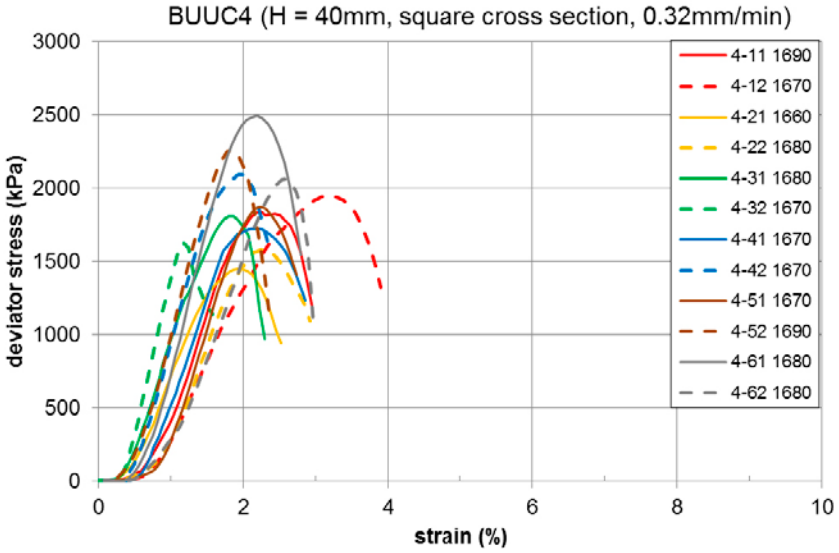

Figure A3-4. *Deviator stress as a function of strain resulting from test series 4 (BUUC4). A total of 12 samples from blocks 1–6 were tested. The deformation rate of the tests was 0.32 mm/min and the specimens had square cross section with a side of 20 mm and a height of 40 mm.*

Appendix 4

Photos of prismatic backfill block specimens from the unconfined compression test series

Figure A4-1. *Post-failure photos from series 1 (BUUC1 – column to the left), series 2 (BUUC2 – the middle column) and series 3 (BUUC3 – column to the right). Each row show photos of samples from the same block, i.e. 7–12, except 8.*

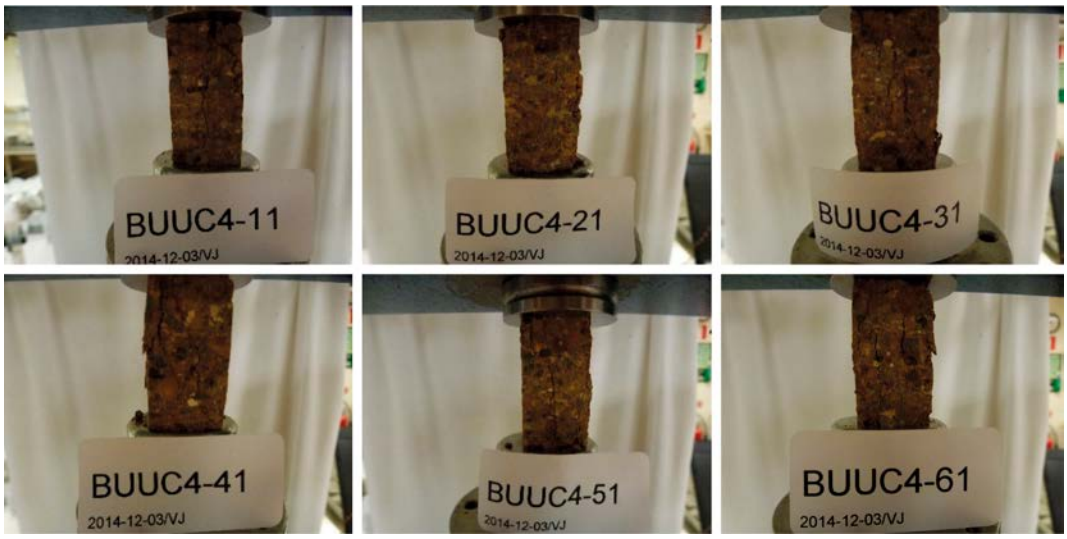

Figure A4-2. *Photos of specimens from blocks 1–6 tested in series 4 (BUUC4).*

Appendix 5

Limited unconfined compression test series with samples of MX-80

A limited test series was made on unsaturated compacted samples of MX-80 to get some indication of the influence of deformation rate, specimen size and form of the cross section. In Figure A5-1 the results from the test series are shown together with a comparable reference line of MX-80 presented by Dueck et al. (2011) in order to take the difference in dry density into account. The reference line was based on results from saturated cylindrical specimens with the diameter 20 mm and the height 40 mm and the specimens were sheared with a deformation rate of 0.32 mm/min.

In the actual test series a total of 10 specimens were sheared. Seven specimens had a circular cross section (with a diameter of 35 mm or 20 mm) and three specimens had a square cross section (with a side of 20 mm). The height of the specimens were double the size of the diameter or the side (in case of square cross section). In the legend of Figure A5-1 the dimensions of the specimens are shown with the size of the diameter or the side (d=35 mm, d=20 mm or s=20 mm). The legend also shows the rate of deformation used (0.32 mm/min or 0.09 mm/min). All specimens were compacted in an oedometer ring with the diameter 20 or 35 mm in three layers (with a third of the total mass of the specimen in each layer) to minimize the difference of density over the specimen. Some of the specimen were then trimmed to a square cross section. The specimens tested had a degree of saturation between 74 % and 84 %, however the influence of degree of saturation in this range has previously been shown to be limited in terms of maximum deviator stress on small specimens of MX-80 (Dueck 2010).

No large deviation from the reference line was seen except from one specimen (one of the red circles) with a circular cross section, diameter of 35 mm, and sheared with a deformation rate of 0.32 mm/min. In addition to the deviating maximum deviator stress at failure for this specimen the density was uncertain and the failure surface looked different compared to the failure surface of other specimens in this project.

Based on this limited series and disregarding the most deviating specimen no further indication of an influence of size and form of the cross section on the maximum deviator stress in unconfined compression tests was noticed.

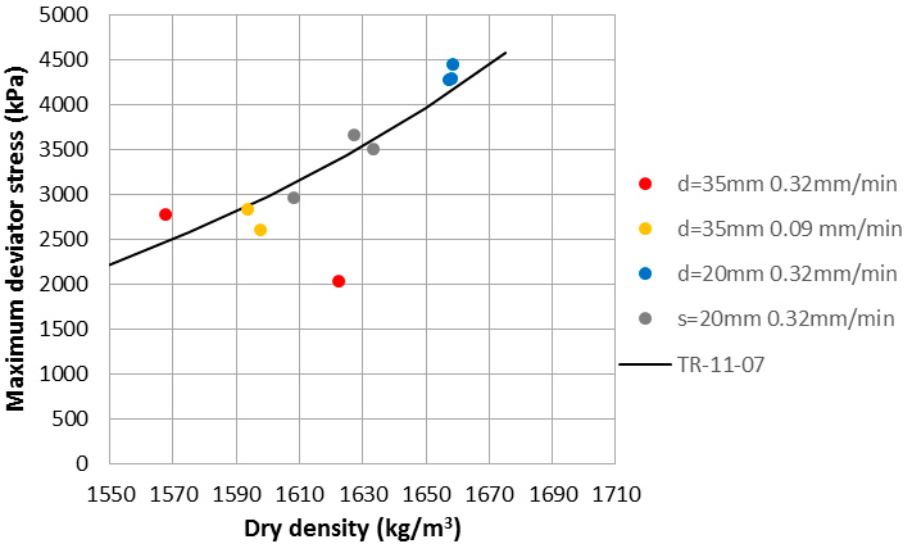

Figure A5-1. *Results from tests on unsaturated specimens of MX-80. The specimens had different cross sections; circular with a diameter of 35 mm or 20 mm (labels: d=35 mm or d=20 mm) or square cross section with the side 20 mm (label: s=20 mm). The specimens were tested with a deformation rate of 0.32 mm/min or 0.09 mm/min as shown in the labels. The results are shown together with a reference line presented by Dueck et al. (2011).*

Arkitektkopia AB, Bromma, 2017

SKB is responsible for managing spent nuclear fuel and radioactive waste produced by the Swedish nuclear power plants such that man and the environment are protected in the near and distant future.

skb.se